AD-A080 524 SYBUCON INC ATLANTA GA F/G 20/4
CALCULATION OF TIMEDEPENDENT FLOWS WITH REVERSAL AND SEPARATION--ETC(U)
JUN 79 J F NASH, R M SCRUGGS DAAG29-76-C-0045
UNCLASSIFIED ARO-14039.1-EX NL

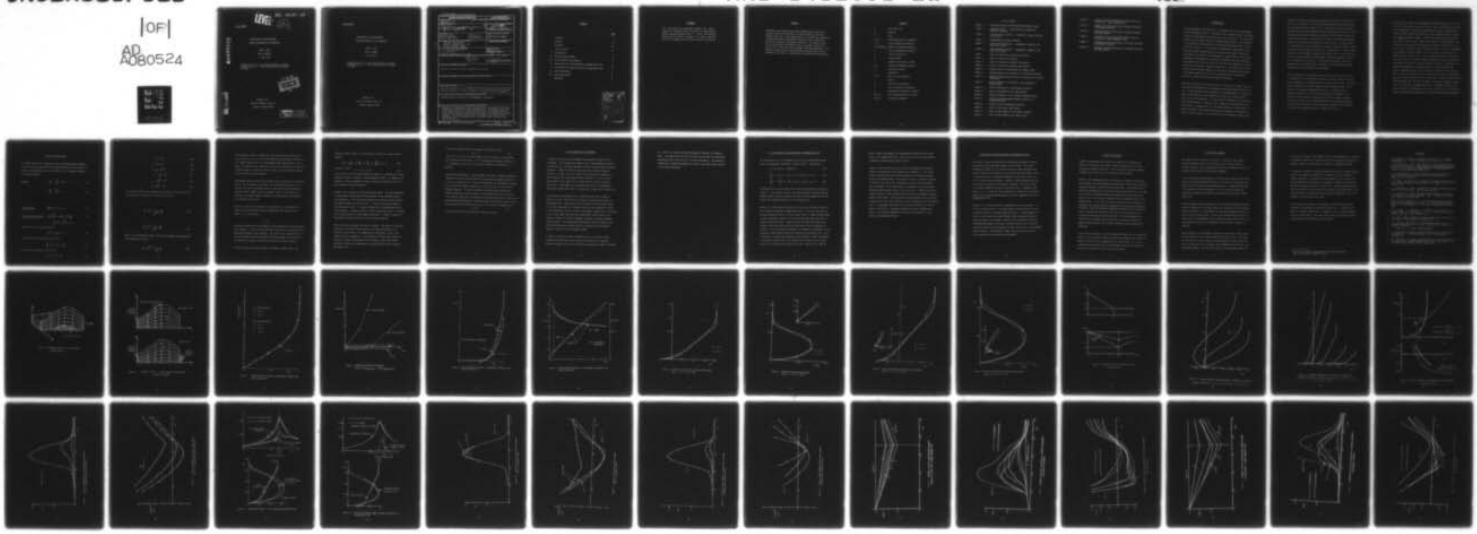

END
DATE FILMED
3-80
DDC

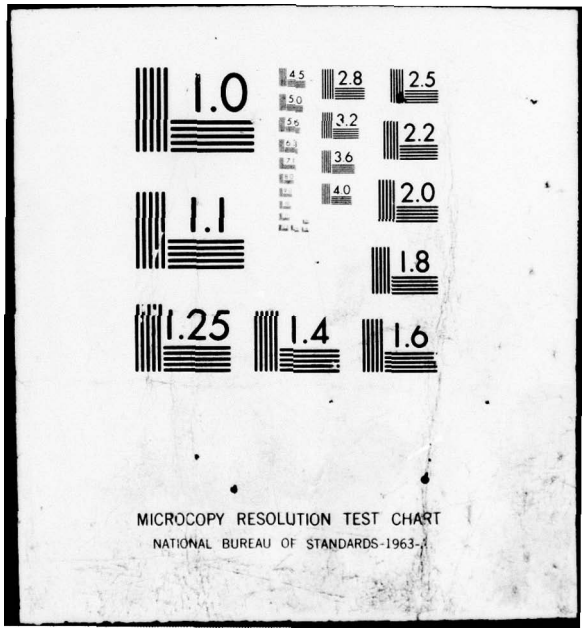
1.0
4.5
5.0
5.6
2.8
3.2
3.6
4.0
2.5
2.2
2.0
1.8
1.1
1.25
1.4
1.6
MICROCOPY RESOLUTION TEST CHART
NATIONAL BUREAU OF STANDARDS-1963-A

FINAL REPORT

CALCULATION OF TIME-DEPENDENT FLOWS WITH REVERSAL AND SEPARATION

JOHN F. NASH

ROY M. SCRUGGS

15 June 1979

Prepared for the U. S. Army Research Office, Research Triangle Park, N.C. 27709, under Contract No. DAAG29-76-C-0045.

Sybucon, Inc.

1900 The Exchange, Suite 175

Atlanta, Georgia 30339

FINAL REPORT

CALCULATION OF TIME-DEPENDENT FLOWS WITH REVERSAL AND SEPARATION

JOHN F. NASH

ROY M. SCRUGGS

15 June 1979

Prepared for the U. S. Army Research Office, Research Triangle Park, N.C. 27709, under Contract No. DAAG29-76-C-0045.

Sybucon, Inc.

1900 The Exchange, Suite 175

Atlanta, Georgia 30339

Unclassified

SECURITY CLASSIFICATION OF THIS PAGE (When Data Entered)

REPORT DOCUMENTATION PAGE

READ INSTRUCTIONS BEFORE COMPLETING FORM

1. REPORT NUMBER: (19) 14039.1-EX
2. GOVT ACCESSION NO.:
3. RECIPIENT'S CATALOG NUMBER:
4. TITLE (and Subtitle): (6) CALCULATION OF TIME-DEPENDENT FLOWS WITH REVERSAL AND SEPARATION
5. TYPE OF REPORT & PERIOD COVERED: (9) Final Report, 15 Jun 76 — 14 Jun 79
6. PERFORMING ORG. REPORT NUMBER:
7. AUTHOR(s): (10) John F. Nash, Roy M. Scruggs (18) ARO
8. CONTRACT OR GRANT NUMBER(s): (15) DAAG29-76-C-0045
9. PERFORMING ORGANIZATION NAME AND ADDRESS: Sybucon, Incorporated, 1900 The Exchange, Suite 175, Atlanta, Georgia 30339
10. PROGRAM ELEMENT, PROJECT, TASK AREA & WORK UNIT NUMBERS:
11. CONTROLLING OFFICE NAME AND ADDRESS: U. S. Army Research Office, P. O. Box 12211, Research Triangle Park, NC 27709
12. REPORT DATE: (11) 15 Jun 79
13. NUMBER OF PAGES: 53
14. MONITORING AGENCY NAME & ADDRESS (if different from Controlling Office): (12) 54
15. SECURITY CLASS. (of this report): Unclassified
15a. DECLASSIFICATION/DOWNGRADING SCHEDULE:

16. DISTRIBUTION STATEMENT (of this Report)

Approved for public release; distribution unlimited.

17. DISTRIBUTION STATEMENT (of the abstract entered in Block 20, if different from Report)

18. SUPPLEMENTARY NOTES

The view, opinions, and/or findings contained in this report are those of the author(s) and should not be construed as an official Department of the Army position, policy, or decision, unless so designated by other documentation.

19. KEY WORDS (Continue on reverse side if necessary and identify by block number)

Boundary layers, turbulence, time-dependence, separation.

20. ABSTRACT (Continue on reverse side if necessary and identify by block number)

Fundamental investigations have been performed on the behavior of unsteady compressible turbulent and laminar boundary-layer, and boundary-layer-like, flows experiencing local reversal and separation. An advanced numerical computational method was used, based on an implicit-ADI numerical integration technique. The computing capability and economy of the method permit a systematic study of the subject flows, from first-order to higher-order representations.

DD FORM 1 JAN 73 1473 EDITION OF 1 NOV 65 IS OBSOLETE

Unclassified 392 927

SECURITY CLASSIFICATION OF THIS PAGE (When Data Entered)

CONTENTS

FOREWORD

This investigation was performed by Sybucon, Inc., under Contract No. DAAG29-76-C-0045, for the U. S. Army Research Office, Research Triangle Park, N. C. 27709. The Technical Monitor was Dr. Robert E. Singleton. Dr. John F. Nash and Dr. Roy M. Scruggs served as joint Principal Investigators.

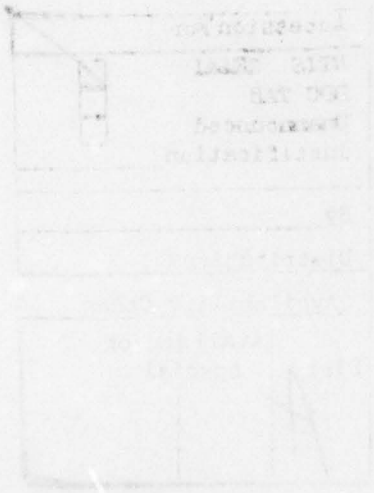

ABSTRACT

Fundamental investigations have been performed on the behavior of unsteady compressible turbulent and laminar boundary-layer, and boundary-layer-like, flows experiencing local reversal and separation. An advanced numerical computational method was used, based on an implicit-ADI numerical integration technique. The computing capability and economy of the method permit a systematic study of the subject flows, from first-order to higher-order representations. The research extended earlier work performed by Sybucon which was also supported by the Army in collaboration with NASA Ames Research Center.

NOTATION

h	total heat flux
p	pressure
t	time
u,v,w	fluctuating velocity components
x,y,z	local orthogonal coordinates
A_1 through A_6	numerical integration matrices
F	vector of dependent variables
G	vector of values of F
H	total enthalpy
L	turbulence dissipation length
P,Q	numerical integration matrices
Q	total mean velocity
T	temperature
U,V,W	mean velocity components
ρ	density
τ_x, τ_z	shear stress components
ε	rate of turbulent dissipation
ν	coefficient of kinematic viscosity
Bar ($\bar{}$)	time averaged quantity or vector
Prime ($'$)	fluctuating component

LIST OF FIGURES

I INTRODUCTION

Unsteady boundary-layer separation is a limiting factor in the performance of many aerodynamic systems: helicopter rotors, turbine blades, the lifting-surfaces of high-maneuverability vehicles, and so forth [1]. The successful design of such systems is far from straightforward because of the complexity of the associated fluid mechanics, and because experimental data are scarce and costly to obtain. In the absence of comprehensive measurements, knowledge of unsteady separating flows is being acquired largely through the intelligent use of numerical experimentation. Again because of the lack of comprehensive measurements, the numerical experiments are being performed using models whose validity can only be inferred by extrapolation of results from other flow regimes: primarily steady flows. The need for this extrapolation places increased emphasis on the need for fundamental correctness in the models themselves, and a certain sophistication of the models is called for, subject to the obvious economic constraints.

Extensive calculations have been carried out, over the last several years, to investigate the properties of time-dependent turbulent boundary layers [2,3,4,5,6]. It has been shown that the effects of time-dependence are to delay the onset of flow reversal in the boundary layer [4], and, in many cases, to delay the onset of separation -- in the sense of detachment of the outer flow from the body surface -- even more [5,6]. Reversal and separation are distinct events, in unsteady flow [7], and between them lies a flow regime in which the boundary layer remains thin despite the presence of reversed flow close to the body surface. The existence of this intermediate regime has an

important bearing on the sequence of events which lead up to dynamic stall [1,8], and it permits the use of first-order boundary-layer theory to study the flow characteristics therein [5,6]. Studies of this latter type have been made for flows which approach separation monotonically [4,5], for flows which are perturbed but subsequently allowed to relax towards steady-state conditions [9], and for oscillatory flows in which the separation-provoking conditions are alleviated during part of each cycle [9]. In flows subject to a progressively severe retardation of the outer inviscid stream, a region of reversal forms and grows in extent with increasing time. As the reversal develops, the displacement thickness grows larger, but it is not until later that a more rapid increase of displacement thickness accompanies the onset of a singularity in the solution. Interesting and important data were generated by all of these studies, leading to an increasing body of knowledge about the reversal/separation phenomenon.

With the intention of elucidating the details of the flow in the vicinity of separation, some calculations were done for unsteady laminar flow using the two-dimensional, incompressible Navier-Stokes equations [9]. The Navier-Stokes equations do not become singular, when separations occurs, but do portray the increasing displacement thickness in situations where a singularity appears in the first-order boundary-layer equations. The results of the calculations using the Navier-Stokes equations helped to clarify the solutions of the turbulent boundary-layer equations obtained earlier, and also served to relate the work on turbulent flows at Sybucon to studies made elsewhere for purely laminar flows [10, eg.].

The work done by Sybucon on time-dependent turbulent boundary layers, up to the time of the present study, was all done using a calculation method based on the integration of the partial differential equations, together with a turbulence model involving the turbulent kinetic-energy equation, by means of an explicit numerical scheme. Although the method served to provide a wide range of useful results, significant weaknesses became apparent. One of these was the necessity for matching the numerical solution to the Law of the Wall in the region close to the body surface. The use of approximate relationships in the wall region -- which is crucially important to the dynamics of the reversed flow -- was of increasing concern. Another weakness was the use of an explicit numerical scheme which leads to excessively long computer run-times for flows of practical interest. Furthermore, the internal determination of integration step size, necessitated by the explicit formulation, made it more difficult to describe certain types of flow -- notably oscillatory flows -- than would be the case if the temporal node points could be specified freely by the user. Another limitation in the existing method (not, this time, related to the explicit numerical scheme) was its restriction to incompressible flows. Aerodynamic systems rarely operate in purely incompressible flow, and it was felt to be of interest to explore the effects of compressibility on unsteady reversal and separation.

II THE CALCULATION METHOD

The method involves the integration of the following governing equations, in which x and z are measured in the developed surface of the cylinder (x normal to the generators, and z along them), and y is measured normal to the developed surface:

momentum

$$\rho \frac{DU}{Dt} - \frac{\partial \tau_x}{\partial y} + \frac{\partial \rho}{\partial x} = 0 \tag{1}$$

$$\rho \frac{DW}{Dt} - \frac{\partial \tau_z}{\partial y} = 0 \tag{2}$$

thermal energy

$$\rho \frac{DH}{Dt} - \frac{\partial}{\partial y}(h + Q\tau) = 0 \tag{3}$$

turbulent kinetic energy

$$\rho \frac{D}{Dt}\left(\frac{\overline{q^2}}{2}\right) + \rho\, \overline{uv} \frac{\partial U}{\partial y} + \rho\, \overline{vw} \frac{\partial W}{\partial y} + \frac{\partial}{\partial y}\left(\overline{pv} + \frac{1}{2}\overline{q^2 v}\right) + \rho\varepsilon = 0, \tag{4}$$

together with the continuity equation:

$$\frac{\partial}{\partial x}(\rho U) + \frac{\partial}{\partial y}(\rho V) = 0 \tag{5}$$

the definition of the convective derivative:

$$\frac{D}{Dt} = \frac{\partial}{\partial t} + U \frac{\partial}{\partial x} + V \frac{\partial}{\partial y} \tag{6}$$

and the usual peripheral relationships:

$$Q^2 = U^2 + V^2 + W^2 \tag{7}$$

$$\approx U^2 + W^2 \tag{8}$$

$$\tau^2 = \tau_x^2 + \tau_z^2 \tag{9}$$

$$H = C_p T + \frac{1}{2} Q^2 \tag{10}$$

$$\tau_x = \mu \frac{\partial U}{\partial y} - \rho \overline{uv} \tag{11}$$

$$\tau_z = \mu \frac{\partial W}{\partial y} - \rho \overline{vw} \tag{12}$$

$$h = k \frac{\partial T}{\partial y} - \rho \overline{v\phi} \ . \tag{13}$$

The turbulent shear-stress components are assumed to be functions of the turbulent kinetic energy and the mean rate of strain:

$$\overline{uv} = \overline{q^2} f \left(\frac{L}{\overline{q^2}^{1/2}} \right) \frac{\partial U}{\partial y} \tag{14}$$

$$\overline{vw} = \overline{q^2} f \left(\frac{L}{\overline{q^2}^{1/2}} \right) \frac{\partial W}{\partial y} \tag{15}$$

where L is the dissipation length, and the corresponding relationship for the turbulent heat flux is

$$\overline{v\phi} = (\overline{q^2})^{3/2} g \left(\frac{L}{\overline{q^2}} \right) \frac{\partial T}{\partial y} \tag{16}$$

The dissipation length is assumed to be the usual prescribed function of y/δ_E; however, δ_E is not now the local boundary-layer thickness itself, but is a length related to it via a rate equation whose characteristic time is $6\delta/Q_e$. The effect of the introduction of this rate equation is to place the turbulence model on essentially the same status as the two-equation models used by several other investigators.

Experimental data for steady flow indicates that the function f, in Equations (14,15), can be assumed to be linear. The corresponding form for g, in Equation (16), can be determined from f by specifying the distribution of turbulent Prandtl number across the boundary layer. In the present calculations this Prandtl number is taken to be a constant, but the method is not restricted to this form.

The above equations are formulated for turbulent flow. Calculations for laminar flow are performed simply by suppressing the turbulent kinetic energy, i.e., by specifying

$$\overline{q^2} = 0,$$

whereupon the equations become identical to the compressible laminar boundary-layer equations. It will be noted that the viscous terms are retained in the momentum and thermal energy equations. The solution for turbulent flow is continued through the viscous sublayer to the body surface; the solution is not matched to a separate inner-layer calculation in the wall region.

The four principal governing equations (2 momentum, thermal energy, and

turbulent kinetic energy) can conveniently be written as a matrix-vector equation:

$$A_1 F + A_2 \frac{\partial F}{\partial t} + A_3 \frac{\partial F}{\partial x} + A_4 \frac{\partial F}{\partial y} + A_5 \frac{\partial^2 F}{\partial y^2} + A_6 = 0, \qquad (18)$$

in which F, where

$$F^T = \{U, W, T, \overline{q^2}\}, \qquad (19)$$

is the vector of the principal dependent variables, A_1 through A_5 are square matrices of order 4, and A_6 is a four-dimensional vector. A_1 through A_6 are functions F, but are regarded as known, at any given iteration level, via the customary linerization process.

Equation (18) is solved in a three-dimensional domain: two space dimensions, x,y describing a plane normal to the generators of the cylinder, and the time dimension, t. The calculation advances in the positive time direction yielding the complete solution in the x - y plane at each step (Figure 1). The node points in the x - y plane are scanned by an alternating-direction (ADI) technique: a partial solution is first sought along lines x = constant, and a revised solution is then sought along lines y = constant, (Figure 2). One complete iteration consists of a scan in each direction.

There are several advantages of the ADI technique: the number of iterations required is a relatively weak function of the node-point density, the stability of the scheme is not compromised by ambiguities in sign of the chordwise velocity component: U, and extension to higher-order systems of equations is readily accomplished (an ADI scheme is used in the method developed at Sybucon for integrating the unsteady Navier-Stokes equations; see Reference 9).

For a scan in either direction, Equation (18) takes the form

$$PG = Q \tag{20}$$

where the G is the vector whose elements are the values of F at each node point along the line of scan. P is a tridiagonal matrix whose elements are 4 x 4 submatrices, and Q is a vector whose elements are themselves 4 x 1 matrices.

Second-order differencing is used throughout the method. Backward differences (relative to the local flow direction) are used for the diagonal elements of A_3 and A_4, in Equation (18), and central differences for the diagonal elements of A_5 and the off-diagonal elements of A_4 (A_3 and A_5 have no non-zero off-diagonal elements). In order to preserve the second-order status of the backward differences, two node points, at the current time level, and three at the previous time level, are involved in each representation of a derivative. The differencing arrangement is chosen primarily for stability reasons, but it offers good precision characteristics also. The solution of Equation (20):

$$G + P^{-1}Q \tag{21}$$

yields the solution for the particular scan and iteration.

III THE VALIDATION OF THE METHOD

A range of calculations was performed to establish the credibility of the method. For two-dimensional laminar flow a time-relaxation solution was found to be in excellent agreement with the classical Blasius solution (Figure 3). Numerical solutions were derived for various node-point densities, as shown, and it is evident that satisfactory convergence is being achieved with second-order accuracy (Figure 4); an error in wall shear stress of less than 0.2% is incurred with as few as 11 vertical node-points. Some comparison calculations show that the corresponding first-order computations result in substantially larger errors (Figures 3,4).

A time-relaxation calculation for a steady turbulent flow is shown in Figures 5,6, and a typical level of accuracy is achieved with respect to experimental data. With regard to the validation of the turbulence model is is worth mentioning that a separate study has been conducted to verify a three-dimensional "steady" version of the present method [13]. The results of this study showed that some small improvements could be made to the empirical content of the model although, in general, the model performed reasonably well. The corresponding improvements were not included in the present method because of doubts about the invariance of the proposed changes to rotation of the coordinate system.

In order to examine the effect of grid density on the solution, under reversed-flow conditions, some calculations were done for a retarded turbulent boundary layer, and the results are presented in Figures 7 through

10. The flow is similar to those considered in Sections III through V, below. The comparisons show that the details of the flow are represented surprisingly well even with only 11 vertical node-points. The remaining calculations, presented throughout this report, were done using 21 points in the vertical direction.

IV CALCULATIONS FOR TWO-DIMENSIONAL INCOMPRESSIBLE FLOW

The calculations were all performed for the class of prescribed external velocity distributions described as "frozen flows"[9]. Specifically

$$U_e = U_o, \text{ for } t \leq o \text{ and all } x, \tag{22}$$

$$\frac{U_e}{U_o} = 1 - \frac{x}{x_1}\{1 - f(t)\}, \text{ for } t \geq o \text{ and } o \leq x \leq x_1, \tag{23}$$

$$\frac{U_e}{U_o} = 1 - \frac{x_2 - x}{x_1}\{1 - f(t)\}, \text{ for } t \geq o \text{ and } x_1 \leq x \leq c. \tag{24}$$

The function f(t), and the form of the velocity distribution, are shown in Figure 11. This external velocity distribution imposes an adverse pressure gradient (whose severity increases with time) over the forward part of the chord, and a favorable gradient over the rearward part.

Figures 12, 13 show typical solutions, for this type of velocity field, for both laminar and turbulent incompressible flow. It will be seen that the passage through the point of zero wall shear stress is smooth and uneventful, and that substantial regions of reversed flow develop before the onset of singular conditions occurs. Figure 14 shows the rapid thickening of the boundary layer which takes place some time after the first appearance of reversal. For the particular combination of parameters, in Equations (22-24), singularity onset occurred before the freezing of the external flow. Other calculations, in which these parameters were different, showed the approach to singular conditions after the external flow was frozen, but the divergence of the solution was essentially the same. Figures 15, 16 show the

familiar spacial distributions of displacement thickness and wall shear stress, for incompressible flow. These are similar to the distributions presented in several earlier papers [5,6,9].

Figure 17 shows the effect on the solution of allowing the dissipation length to lag behind the local boundary-layer thickness. It was noted earlier that the inclusion of the rate equation for dissipation lenght raises the turbulence model to two-equation status. As would be expected, the effect of the lag is most conspicuous in regions of rapid boundary-layer thickening. On the other hand, the influence on the velocity and turbulent-kinetic-energy fields is relatively small. Figure 18 shows the results of making a rough correction for the effects of mementum transport normal to the surface. Here the normal pressure gradients were calculated retrospectively after each iteration, and were averaged, across the boundary layer. In subsequent iterations of the solution the effect was reintroduced in the form of a y-dependent modification of the streamwise gradients. The procedure appeared to be stable, and resulted in a small change in the converged solution.

V CALCULATIONS FOR YAWED FLOW AND FOR COMPRESSIBLE FLOW

The effect of yaw on the solution was investigated by adding a constant W-component to the prescribed external velocity field. The results presented in Figures 19, 20, which are typical of those obtained, show that the effect on the chordwise velocity field within the boundary layer is relatively minor. The spanwise component of wall shear stress does not, of course, reverse although it exhibits a shallow minimum near the first point of reversal of the chordwise component. The angle between the external streamlines and the x-axis varies with x, reaching a maximum at $x = x_1$. At the time level represented in Figure 20, this maximum angle is 63°, while the maximum angle of the wall streamlines is in the neighborhood of 135°.

Figures 21, 22, show the effect of compressibility on the solution. It will be seen that there is a striking change in the distribution of displacement thickness as the Mach number increases. At a Mach number of 3 there is little sign of the rapid boundary-layer thickening which dominates the picture at low speeds. Another, less conspicuous, effect of increasing Mach number is the delay of reversal onset; this is the only significant effect on the distribution of wall shear stress in the neighborhood of reversal. Interestingly, though, these calculations indicate little variation of the position of reattachment.

VI OTHER CALCULATIONS

A number of important calculations were performed to investigate the effects of alleviating the external velocity gradients so as to delay the onset of singular conditions. These calculations have been reported elsewhere [12], and will not be presented in detail herein.

Briefly, it was demonstrated that by judicious alleviation of the chordwise gradients the rapid boundary-layer thickening, indicative of incipient singular conditions, could be delayed indefinitely. The intention was to simulate the modification of the pressure field which occurs in a real flow as the result of coupling between the boundary layer and the outer flow. Typical results are reviewed in Figures 23-28, for laminar as well as for turbulent flow. It will be seen that the alleviation of the gradients is confined to the regions where the singularity would otherwise be expected to develop. With the alleviation mechanism in operation, the calculations could be continued far beyond the point where the calculations in prescribed external velocity fields broke down. The rapid boundary-layer thickening was contained, and the region of reversed flow remained of roughly constant extent as the solution asymptoted towards steady-state conditions.

As was noted in Reference 12, these calculations showed that the singularity onset is not an inevitable feature of first-order boundary-layer theory, but appears to result from an inappropriate use of the theory: i.e., in prescribed external gradients which do not properly allow for the effects of interaction between the visious and inviscid regions.

VII CONCLUDING REMARKS

The purpose of this research was two-fold: to develop a more comprehensive computation tool for the particular class of flows than was hitherto available, and to demonstrate the use of the method as part of an ongoing study of specific fluid-dynamic phenomena.

The new calculation method appears to be firmly based, both from the standpoint of the underlying physical model and in terms of the numerical techniques used to integrate the governing equations. Although the validation of the method has not been extensive, tests run to date indicate that acceptable accuracy and reliability can be achieved at reasonable computation cost.

The fluid-dynamic studies conducted by the new calculation method included parallel computations of unsteady laminar and turbulent flows with embedded regions of reversal. A broad measure of similarity emerged from the solutions in the two types of flow. As was to be expected from the results of earlier work, the development of the solution for either type of flow, was interrupted by the onset of a singularity some time after reversal was observed.

Some calculations were performed to investigate the effects of Mach number, and the effects of yaw, on the development of reversed flows. Yaw seemed to have relatively little effect on the development of the chordwise flow, but, of course, gave rise to spanwise flow components which have their own interesting dynamics. The principal effect of increasing Mach number was

o reduce the thickness of the boundary layer in the neighborhood of reversal; at supersonic speeds only a limited build-up of displacement thickness was observed, whereas a rapid build-up is familiar in incompressible flow.

A significant outcome of the present research has been the observation that onset of the separation singularity in unsteady flow can be delayed, or avoided altogether, by alleviation of the gradients in the external flow. The alleviation of the gradients was intended to simulate the interaction between the boundary layer and the outer flow. The calculations indicated that the singularity onset could be delayed more-or-less indefinitely, and that conditions of steady-state reversal could be approached by way of an asymptotic calculation for long times.*

The new calculation methoc will presumably be used for continued basic research on the mechanics of unsteady reversed flows. In addition the method is currently being used as a component tool in a study of unsteady flow over finite wings. This latter work is part of an on-going program being supported by the Office of Naval Research.

---

* Here, "long" refers to the physical time represented rather than to the required computation time.

REFERENCES

1. W. J. McCroskey: "Recent Developments in Dynamic Stall," Unsteady Aerodynamics, Vol. 1, Univ. of Arizona (R. B. Kinney, Ed.).

2. V. C. Patel and J. F. Nash, "Some Solutions of the Unsteady Turbulent Boundary Layer Equations," Recent Research on Unsteady Boundary Layers, (Proc. I.U.T.A.M. Symposium, Quebec 1971), A. E. Eichelbrenner, Ed., Presses de L'Université Laval, Quebec 1972.

3. R. E. Singleton and J. F. Nash, "A Method for Calculating Unsteady Turbulent Boundary Layers in Two-and-Three Dimensional Flows," AIAA J. 12, No. 5, May 1974.

4. J. F. Nash, L. W. Carr and R. E. Singleton, "Unsteady Turbulent Boundary Layers in Two-Dimensional Incompressible Flow," AIAA J. 13, No. 2, February 1975.

5. J. F. Nash and V. C. Patel, "Calculations of Unsteady Turbulent Boundary Layers with Flow Reversal," NASA CR-2546, May 1975.

6. V. C. Patel and J. F. Nash, "Unsteady Turbulent Boundary Layers with Flow Reversal," Unsteady Aerodynamics, Vol. 1, University of Arizona (R. B. Kinney, Ed.), July 1975.

7. Sears, W. R. and Telionis, D. P., "Unsteady Boundary-Layer Separation," Recent Research Boundary Layers (Proc. I.U.T.A.M. Symposium, Quebec 1971), E. A. Eichelbrenner, Ed., Presses de L'Université Laval, Quebec 1972.

8. R. M. Scruggs, J. F. Nash and R. E. Singleton, "Analysis of Flow-Reversal Delay for a Pitching Foil," A.I.A.A. 12th Aerospace Sciences Meeting, Paper No. 74-183, February 1974.

9. J. F. Nash, "Further Studies on Unsteady Boundary Layers with Reversal," Final Report, Contract NAS2-8771, February 1976.

10. D. P. Telionis, "Calculations of Time-Dependent Boundary Layers," Unsteady Aerodynamics, Vol. 1, Univer. of Arizona (R. B. Kenney, Ed.).

11. J. F. Nash and R. M. Scruggs (Unpublished Work).

12. J. F. Nash and R. M. Scruggs, "Unsteady Boundary Layers with Reversal and Separation," Unsteady Aerodynamics (Proc. AGARD Symposium), September 1977.

13. J. F. Nash and R. M. Scruggs, "Experimental Verification of an Implicit Three-Dimensional Turbulent Boundary-Layer Code," Final Report, U. S. Air Force Contract F33615-77-C-3116, January 1978.

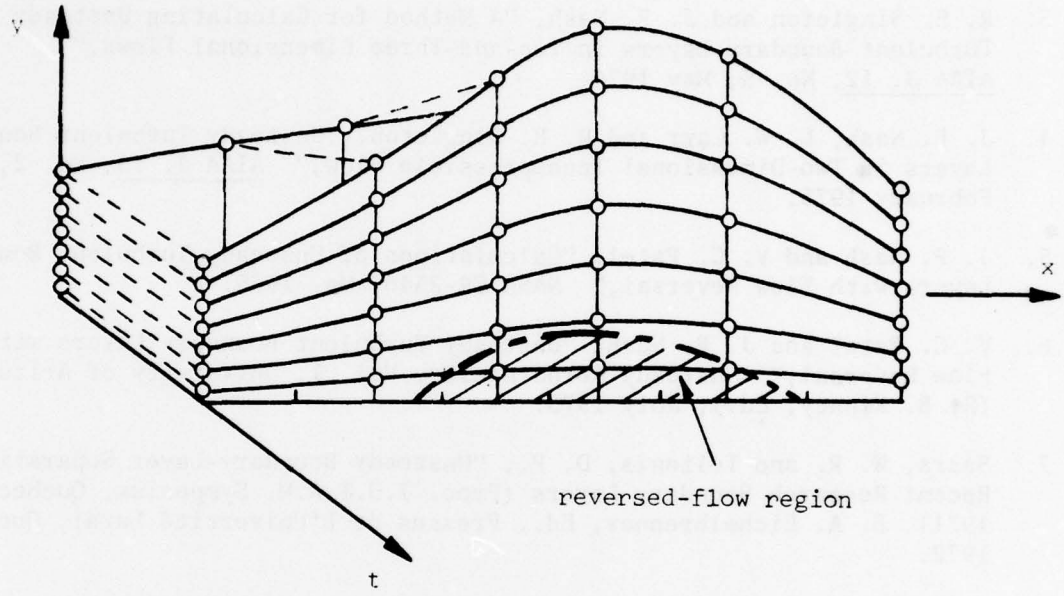

Figure 1 INTEGRATION DOMAIN FOR TIME-DEPENDENT BOUNDARY LAYERS

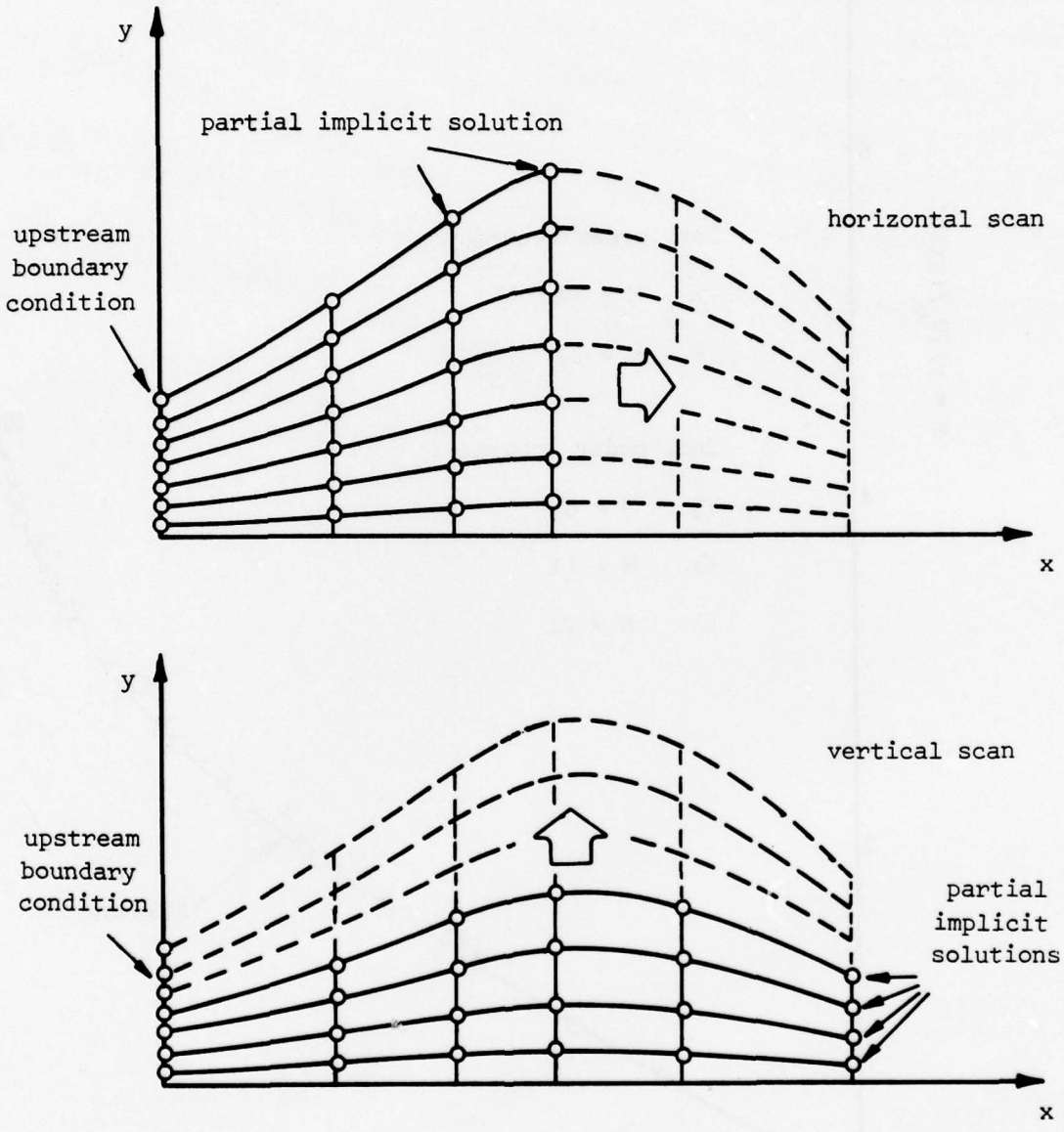

Figure 2 SCANNING OF THE x - y PLANE USING THE ALTERNATING-DIRECTION TECHNIQUE

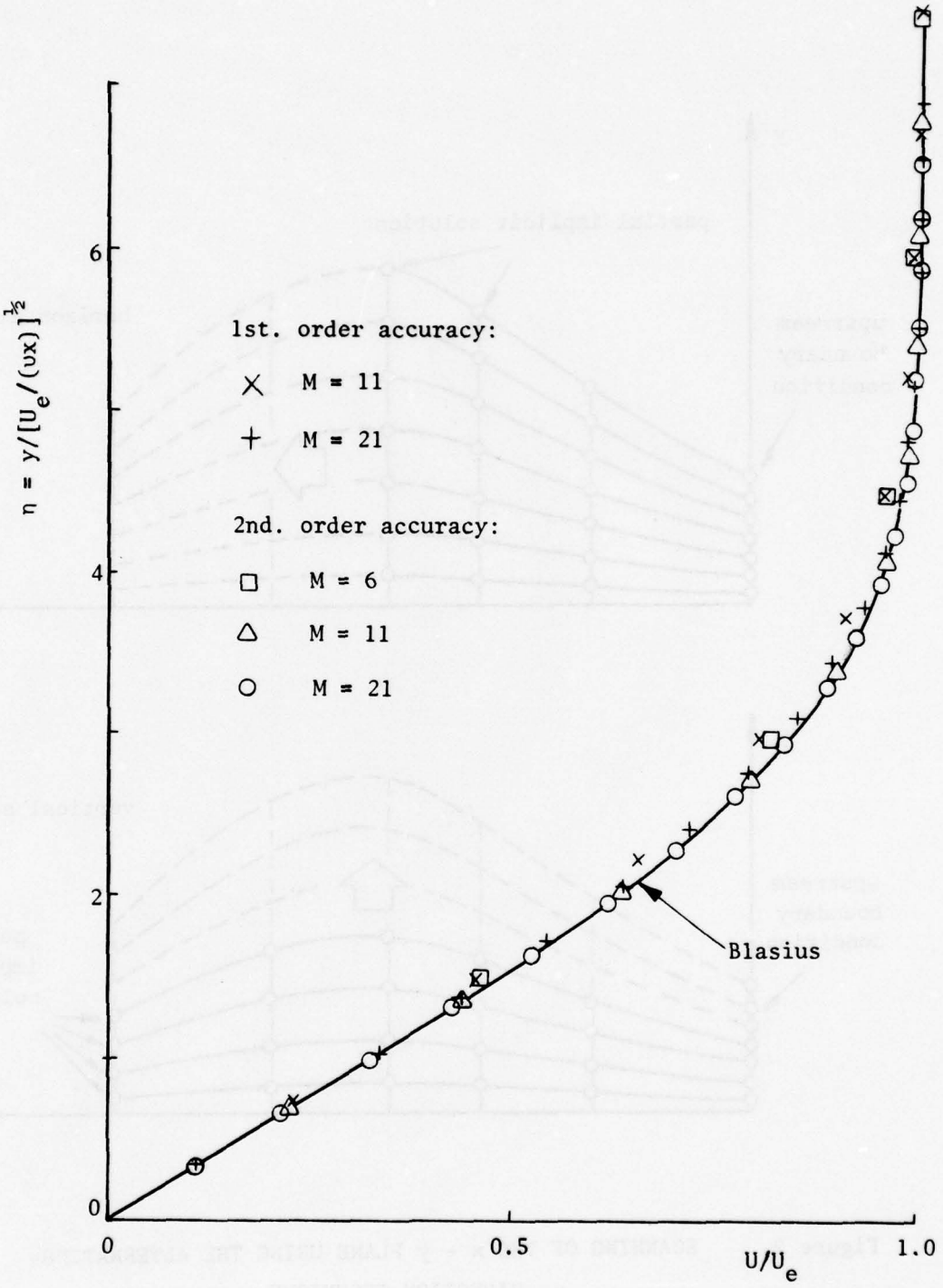

Figure 3 TIME-RELAXATION SOLUTION: 2-DIMENSIONAL LAMINAR FLOW OVER A FLAT PLATE

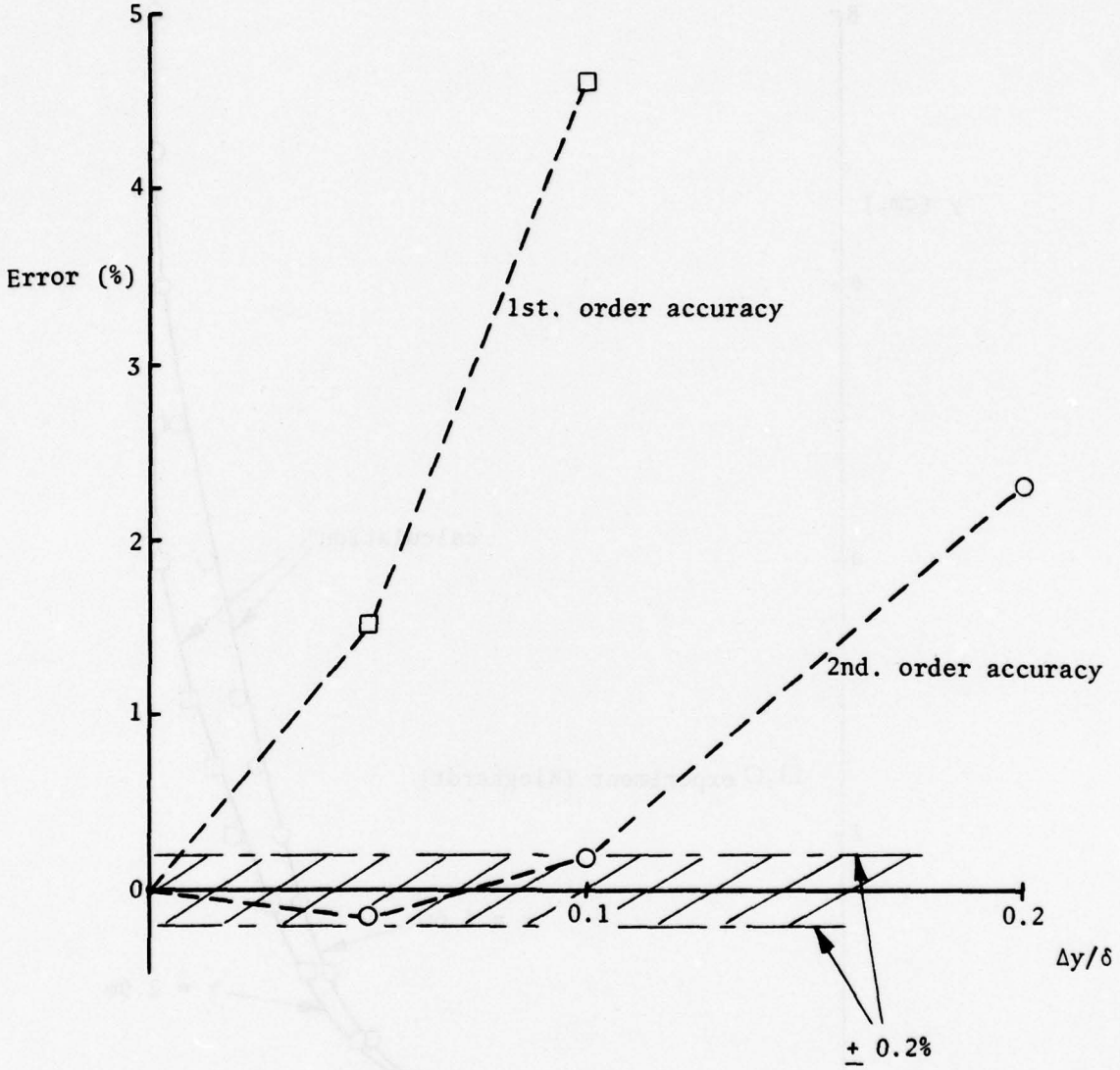

Figure 4 COMPARISON WITH BLASIUS SOLUTION

Error = $[(U/U_e)_{Blasius} - (U/U_e)_{computed}]_{\eta=3}$

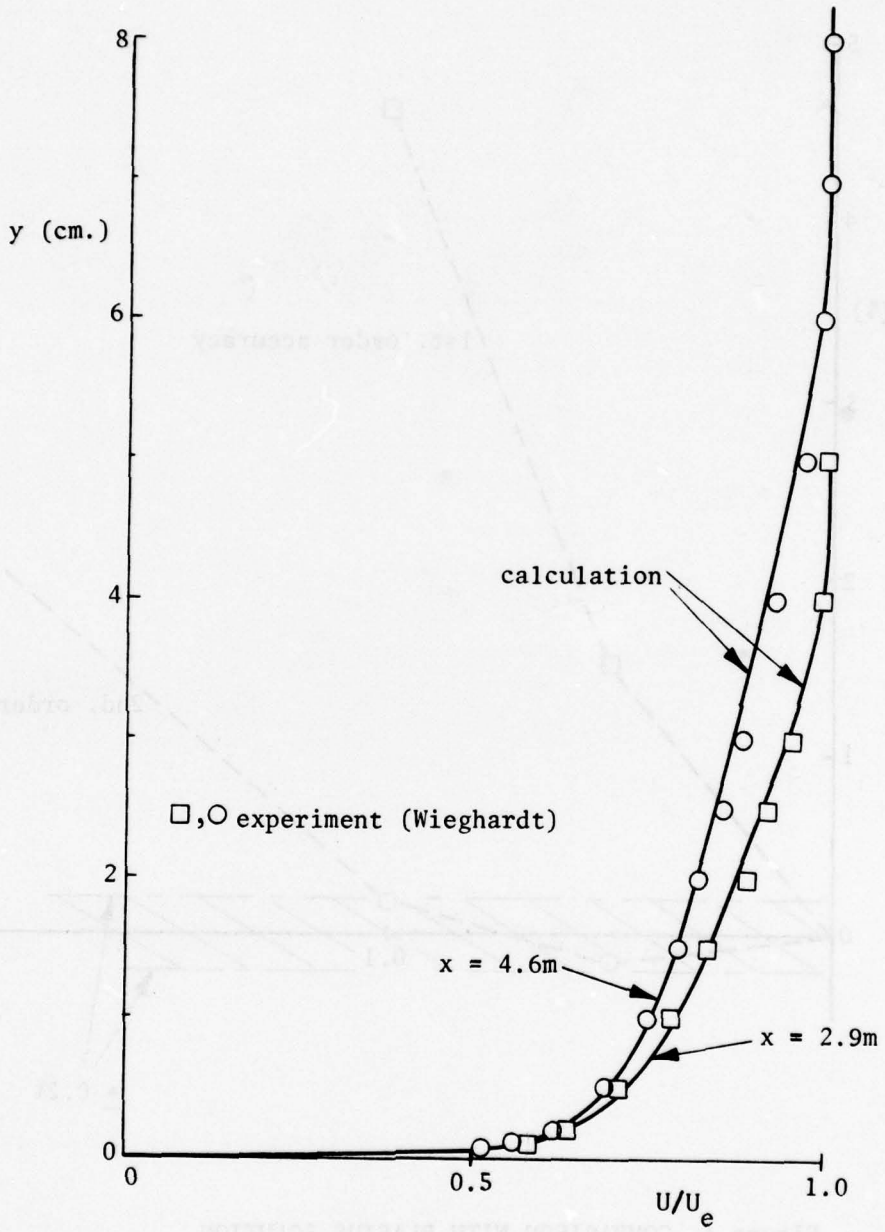

Figure 5 TIME RELAXATION SOLUTION: 2-DIMENSIONAL TURBULENT FLOW OVER A FLAT PLATE

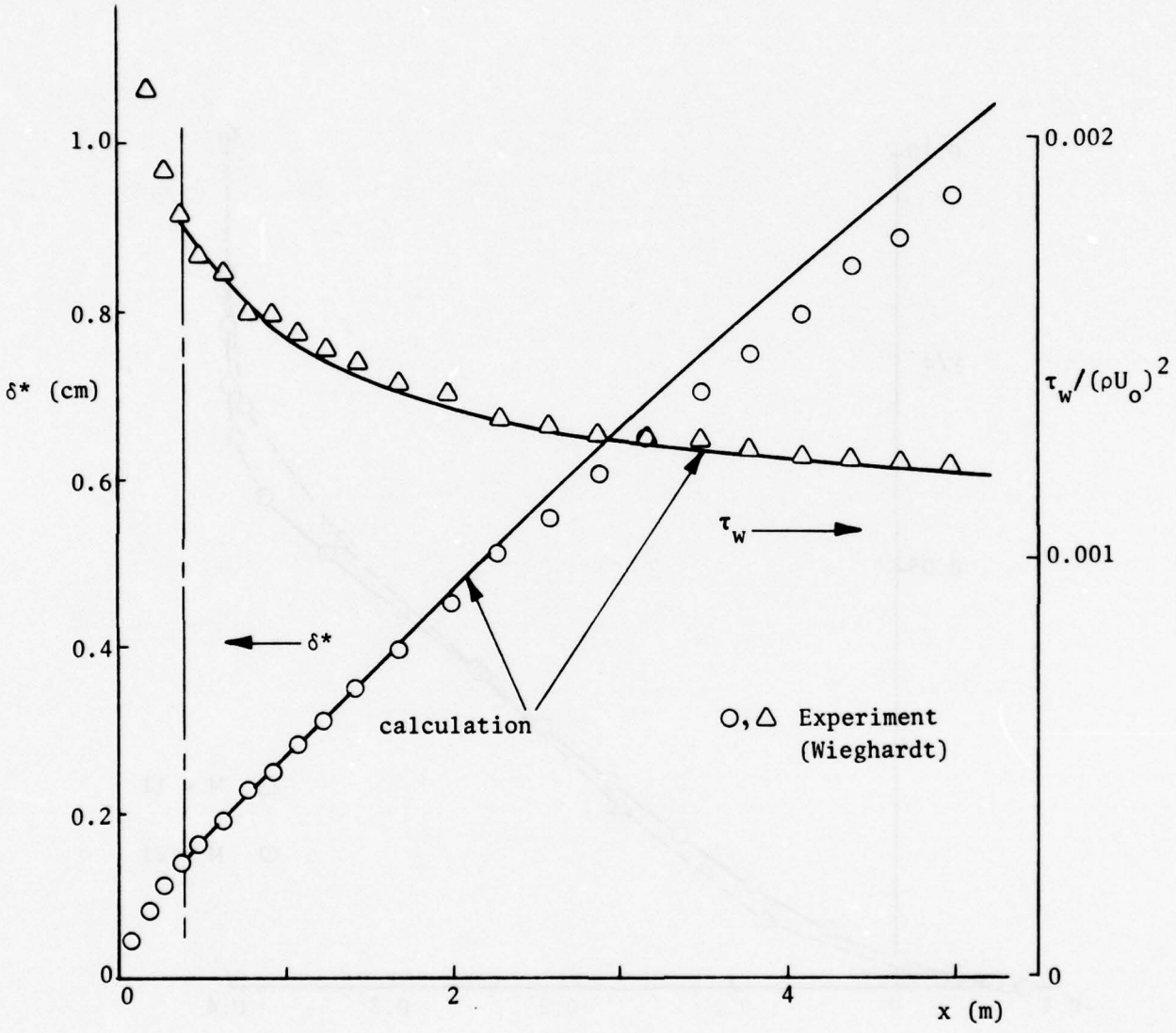

Figure 6 TIME RELAXATION SOLUTION: 2-DIMENSIONAL TURBULENT FLOW OVER A FLAT PLATE

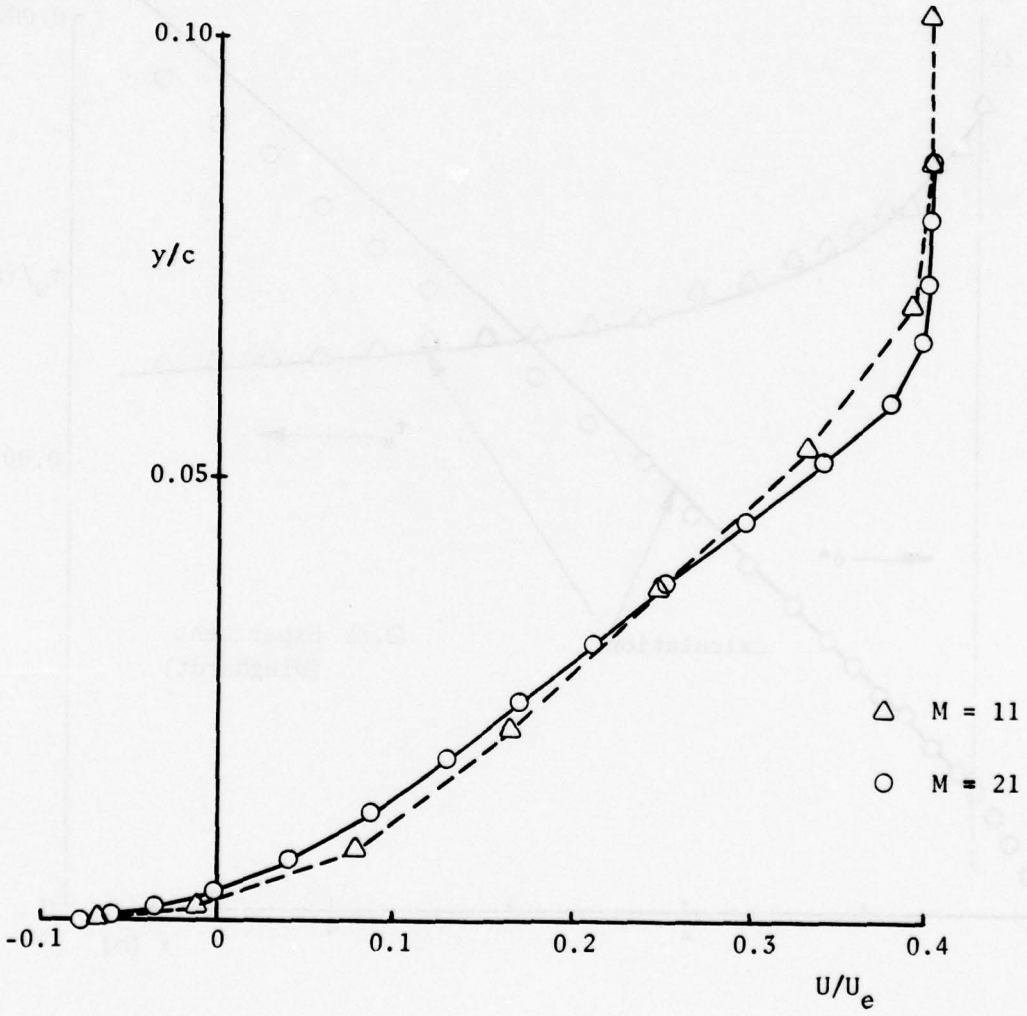

Figure 7 EFFECT OF VARIATION OF VERTICAL GRID DENSITY
[$U_o t/c = 1.3$, $x/c = 0.66$]

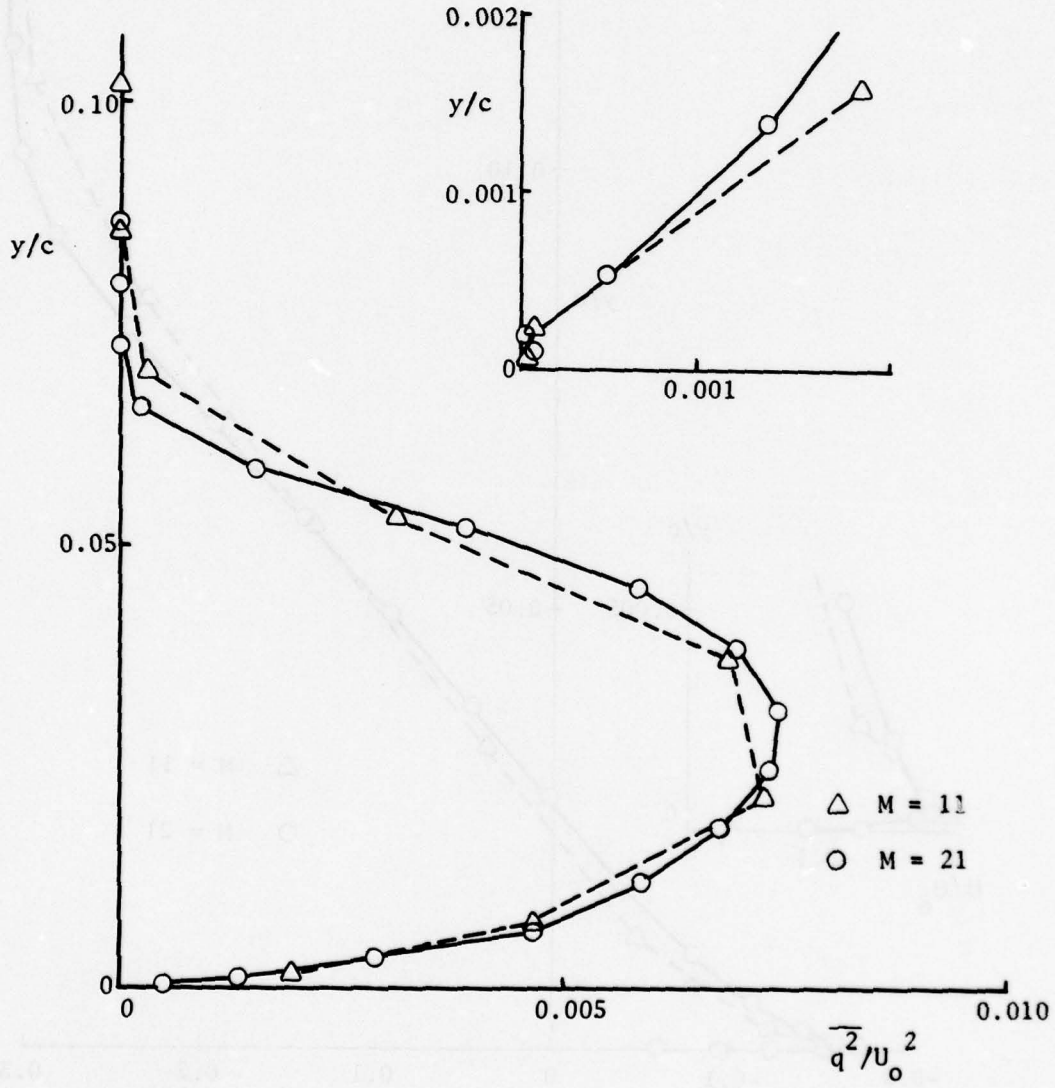

Figure 8 EFFECT OF VERTICAL GRID DENSITY
[$U_o t/c = 1.3$, $x/c = 0.66$]

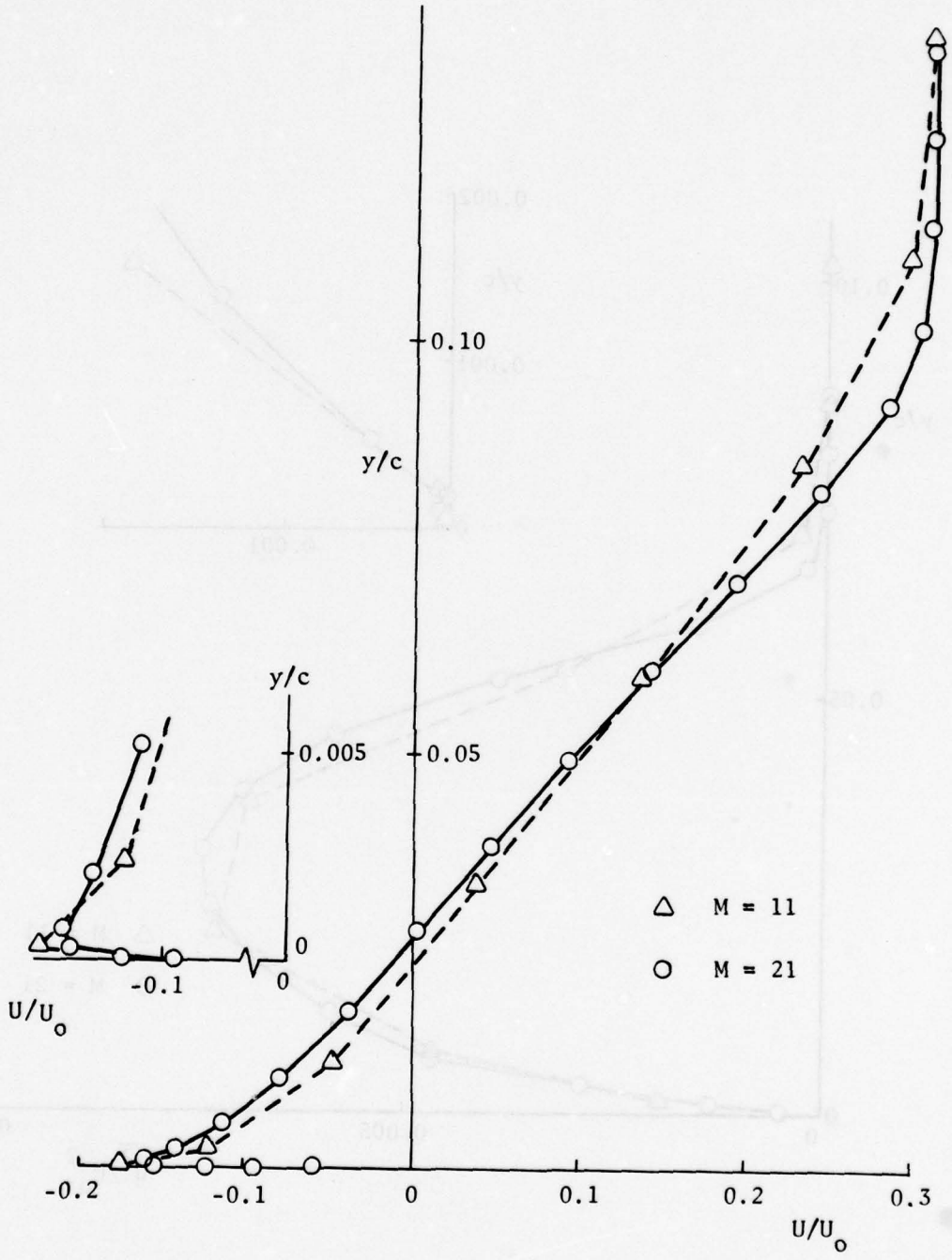

Figure 9 EFFECT OF VARIATION OF VERTICAL GRID DENSITY
[$U_o t/c = 1.5$, $x/c = 0.66$]

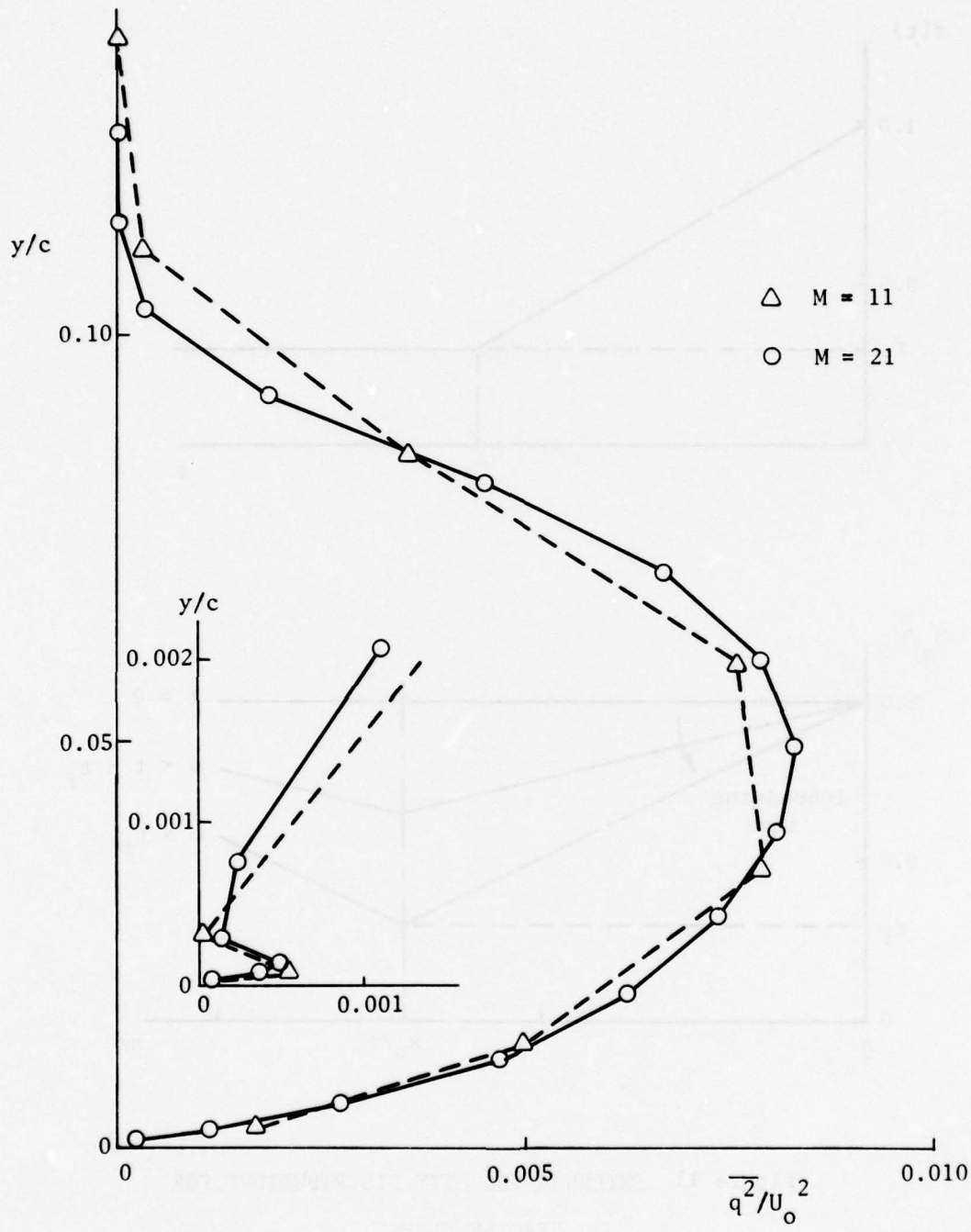

Figure 10 EFFECT OF VARIATION OF VERTICAL GRID DENSITY
[$U_o t/c = 1.5$, $x/c = 0.66$]

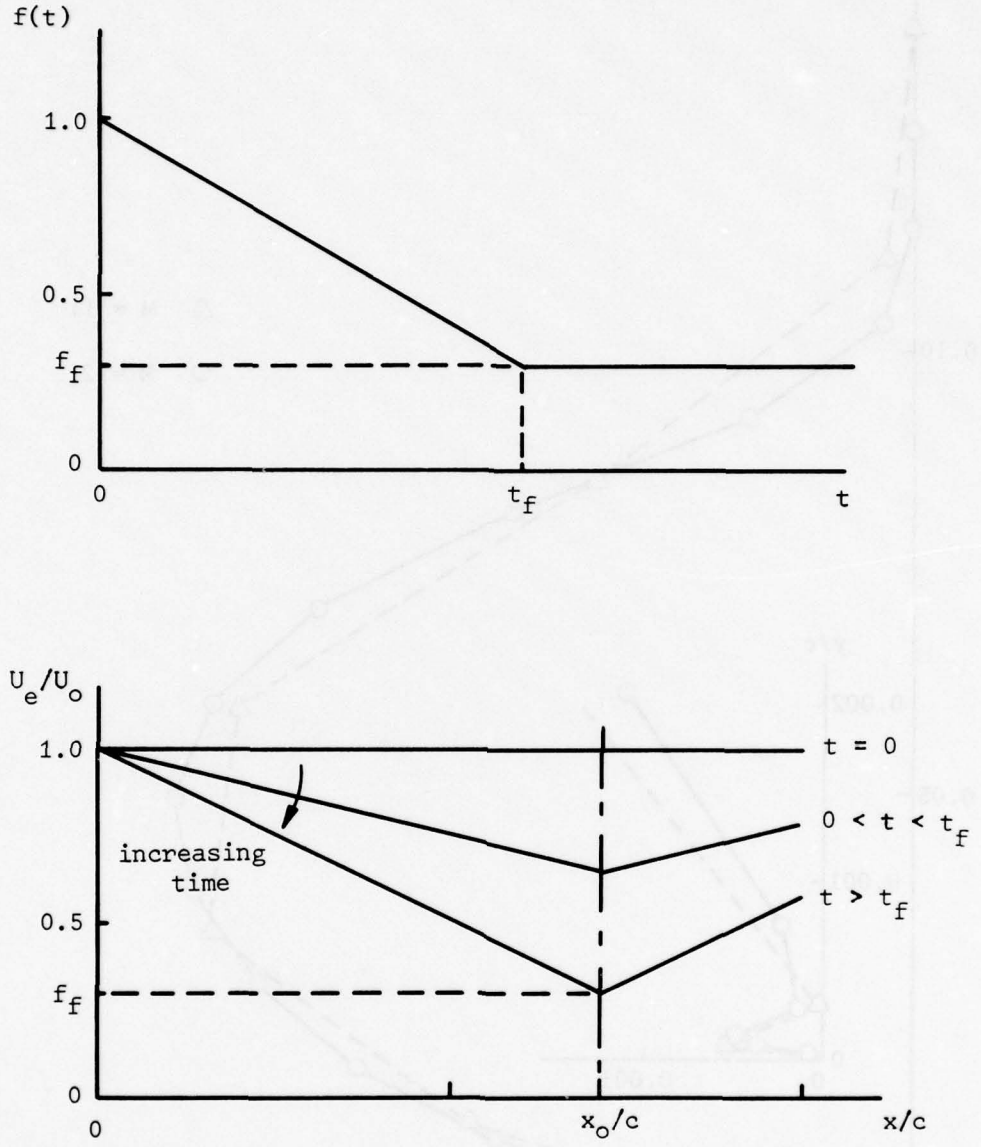

Figure 11 EXTERNAL VELOCITY DISTRIBUTIONS FOR "FROZEN FLOWS"

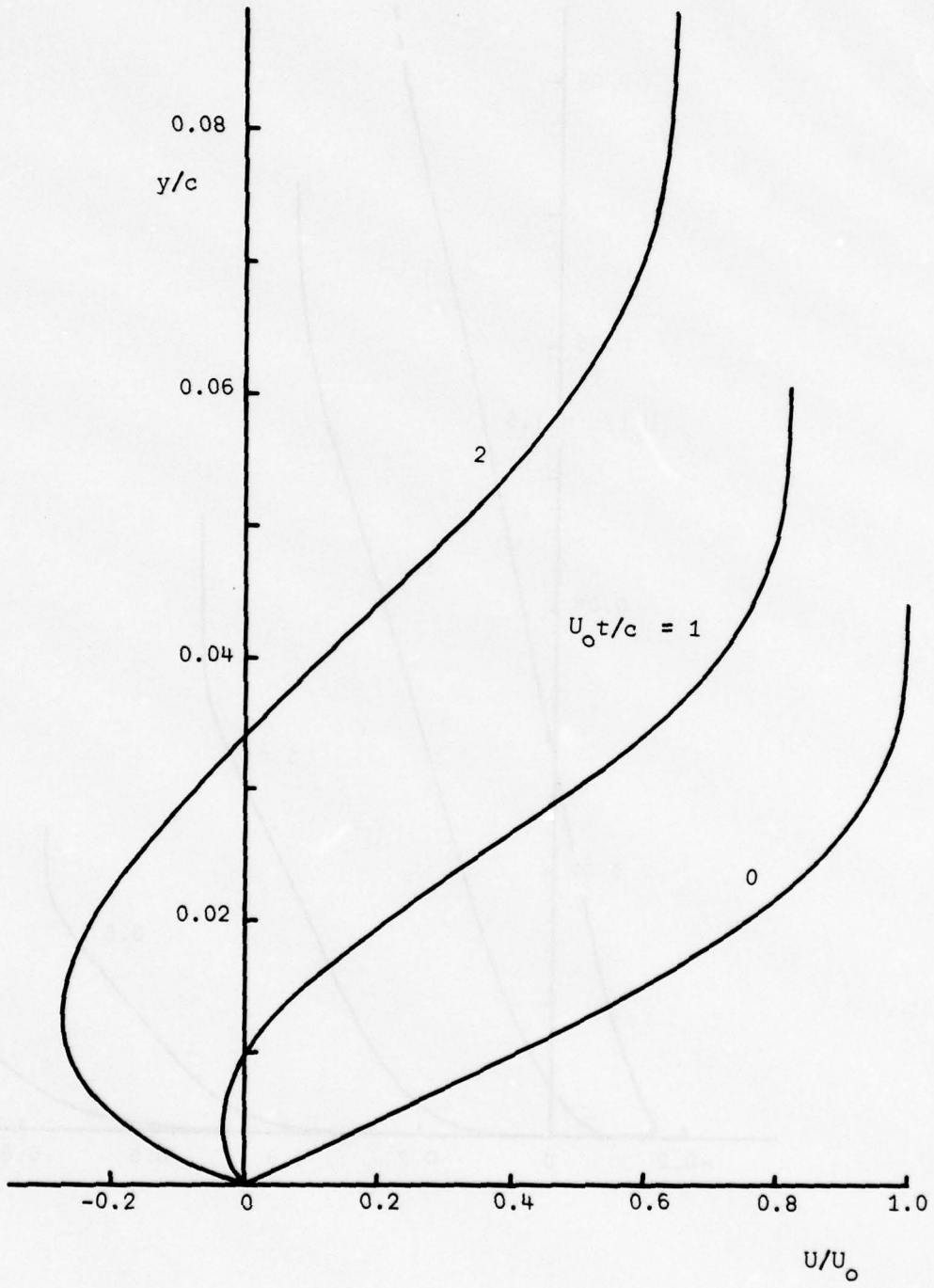

Figure 12 LAMINAR BOUNDARY LAYER PENETRATING A REVERSED- FLOW REGION

(Laminar Frozen Flow: $R_e = 10^4$, $f_f = 0.5$, $t_f = 2.0$, $x/c = 0.5$)

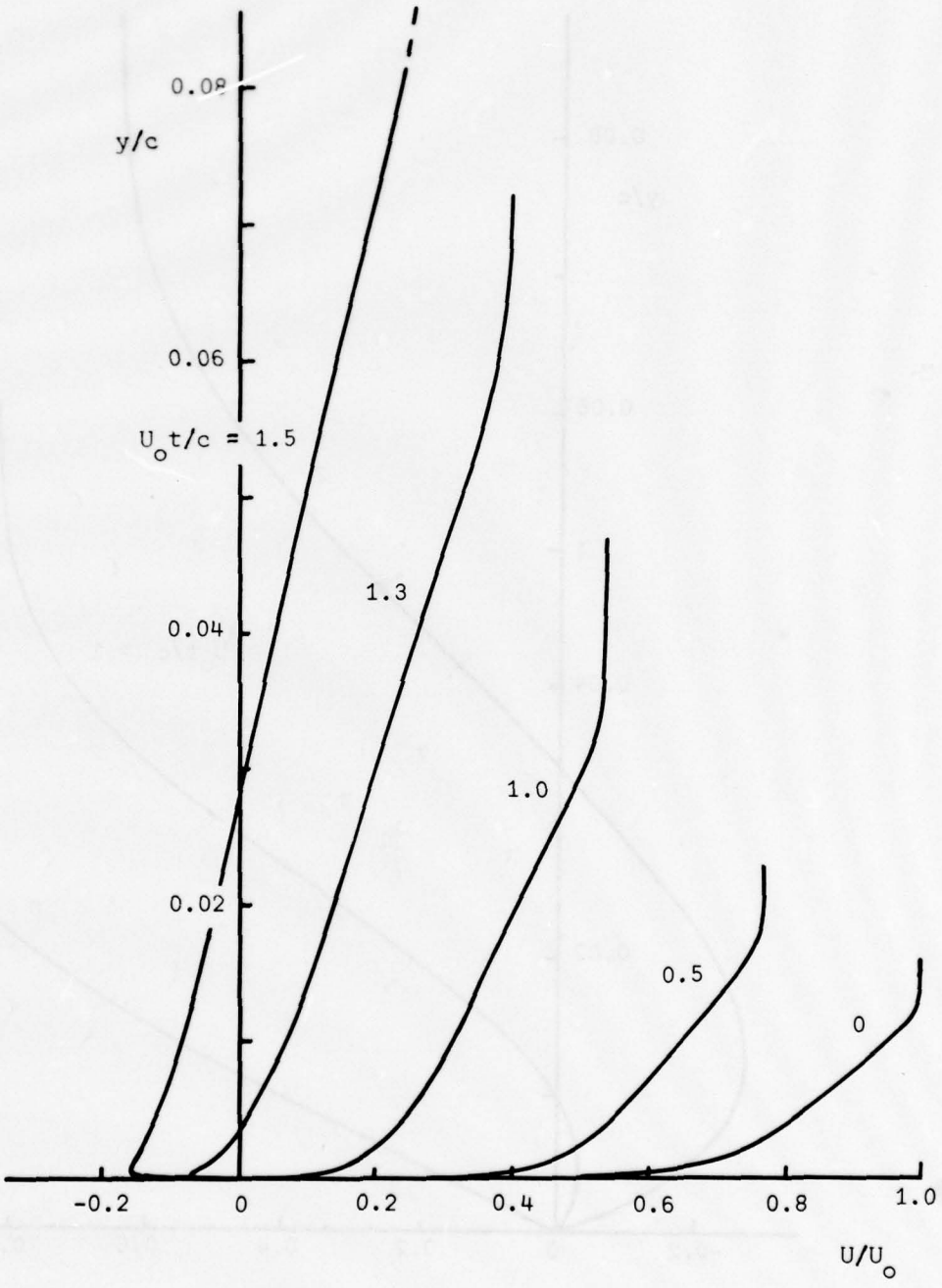

Figure 13 TURBULENT BOUNDARY-LAYER CALCULATION PENETRATING A REVERSED-FLOW REGION (Turbulent Frozen Flow: $R_e = 10^7$, $f_f = 0.25$, $t_f = 1.5$, $x/c = 0.66$)

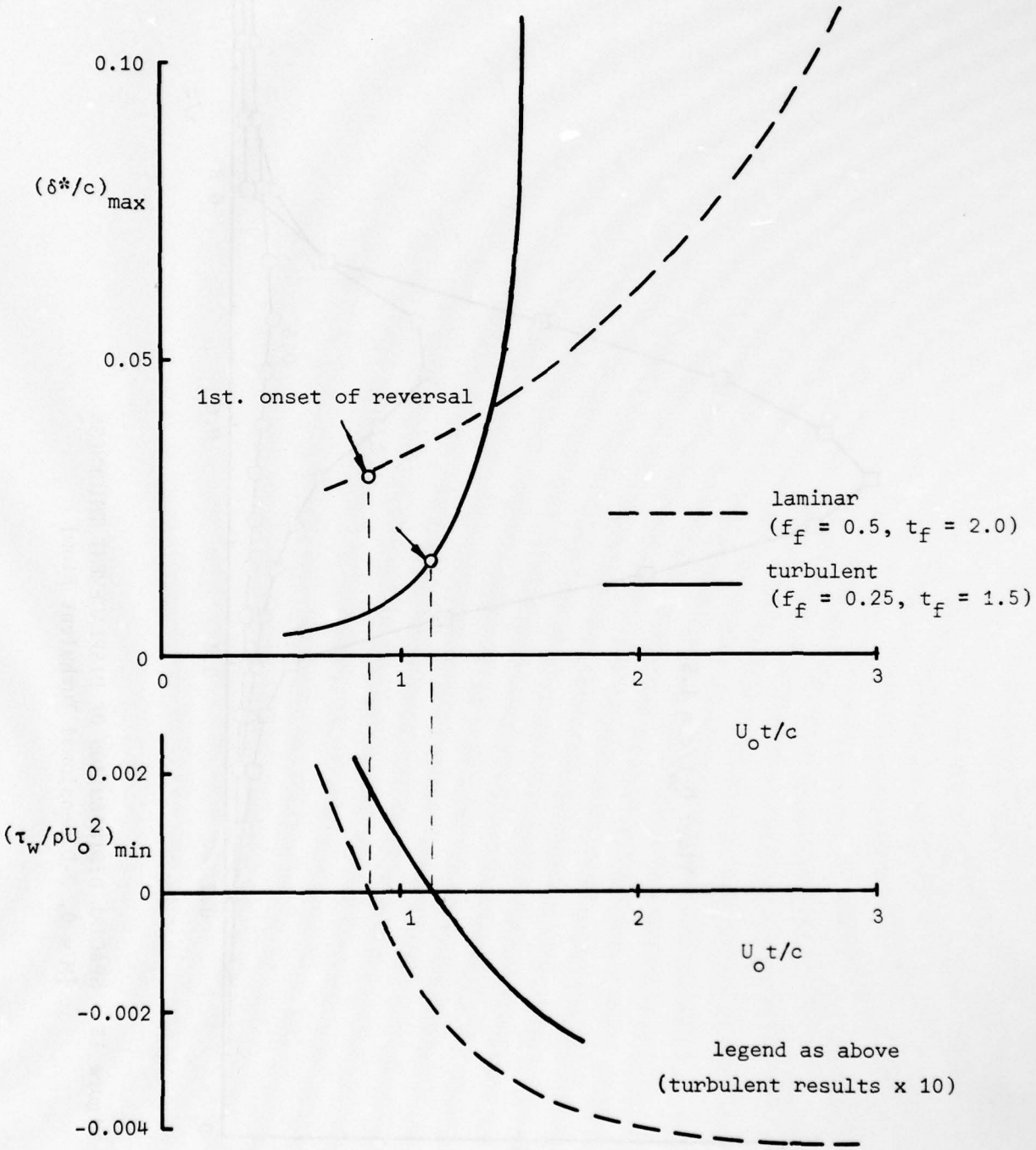

Figure 14 RAPID THICKENING OF THE BOUNDARY LAYER SUBSEQUENT TO REVERSAL ONSET

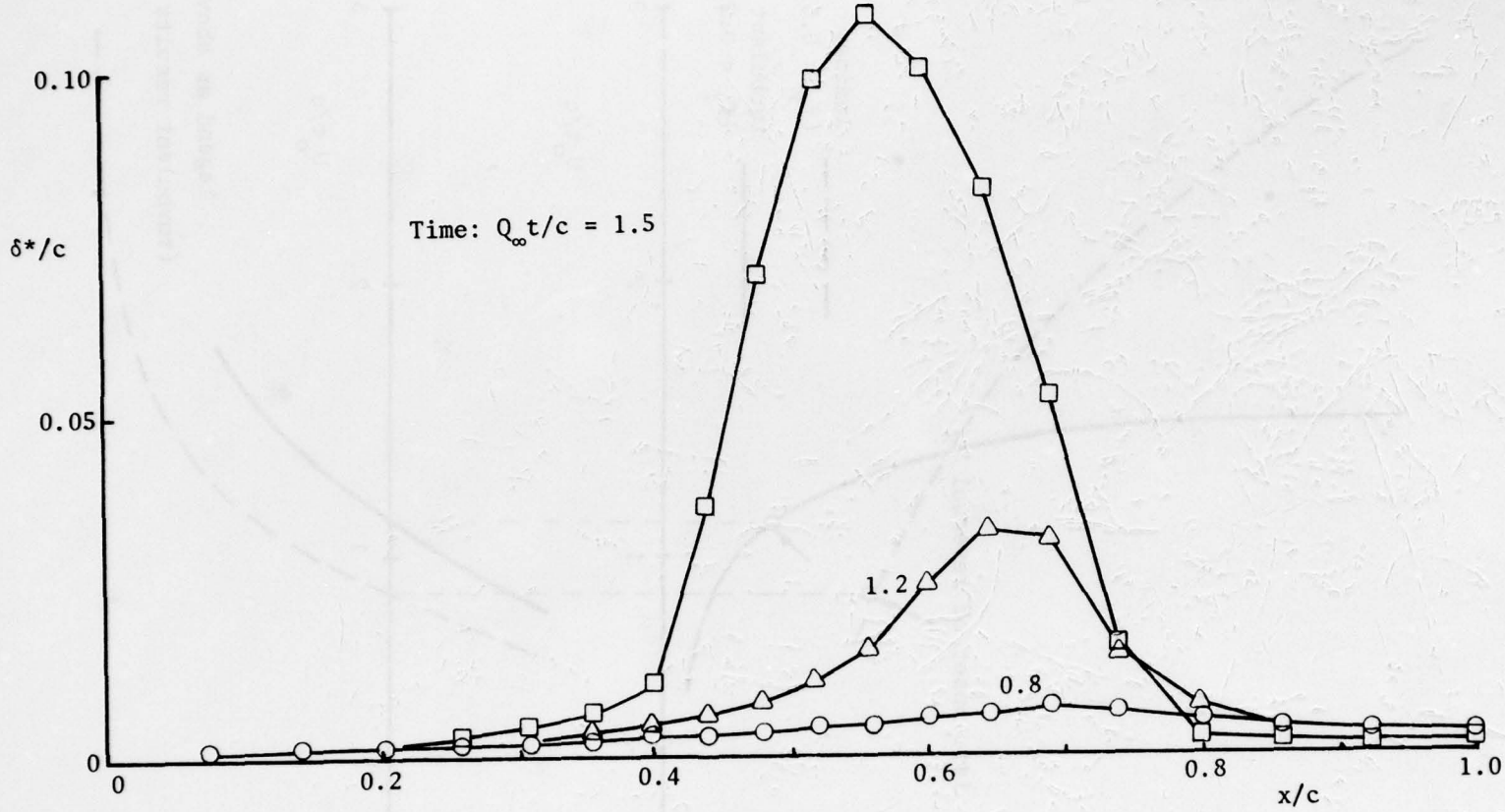

Figure 15 SPACIAL DISTRIBUTION OF DISPLACEMENT THICKNESS
[M = 0, 2-Dimensional Turbulent Flow]

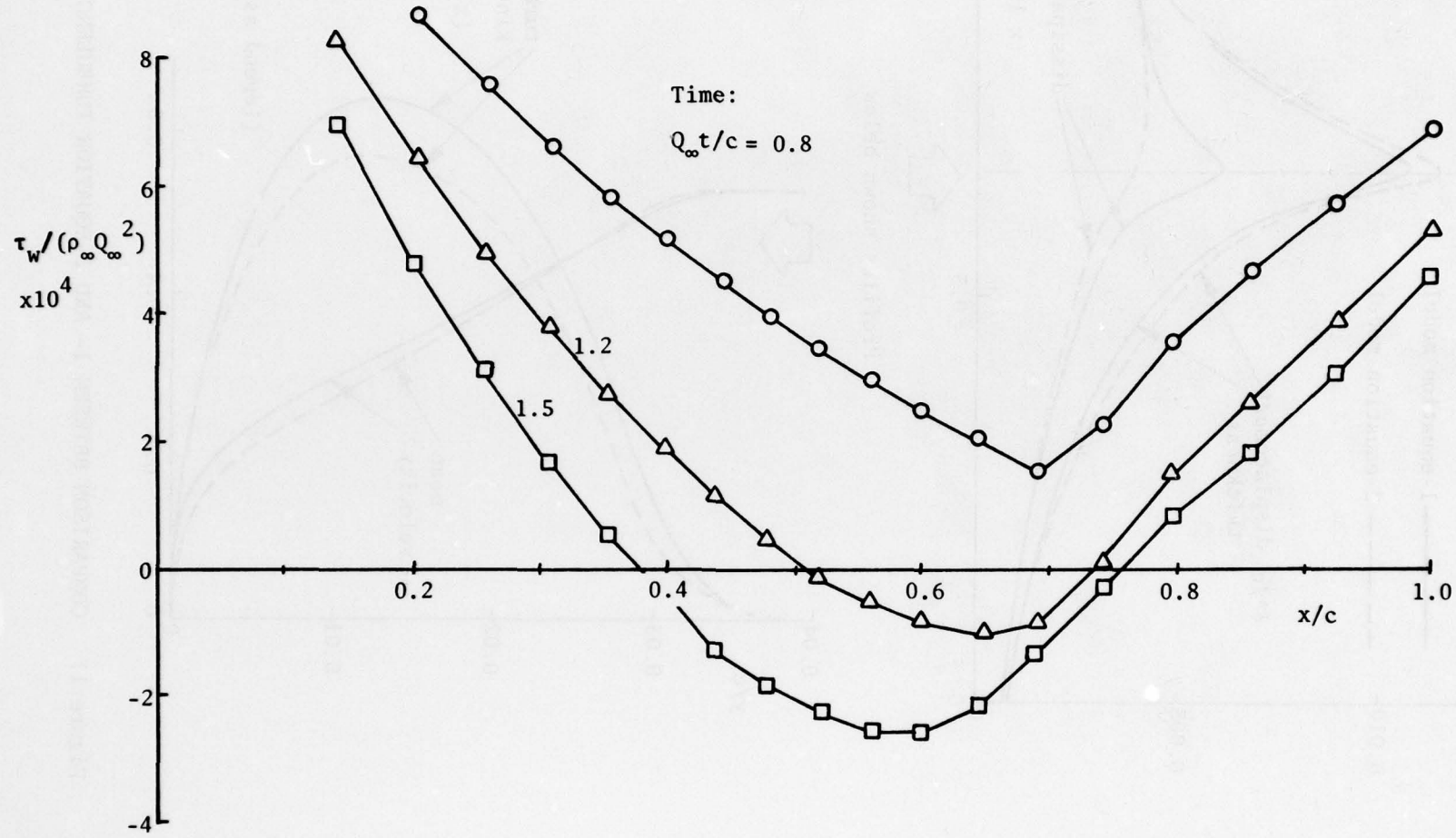

Figure 16 SPACIAL DISTRIBUTION OF WALL SHEAR STRESS
[M = 0, 2-Dimensional Turbulent Flow]

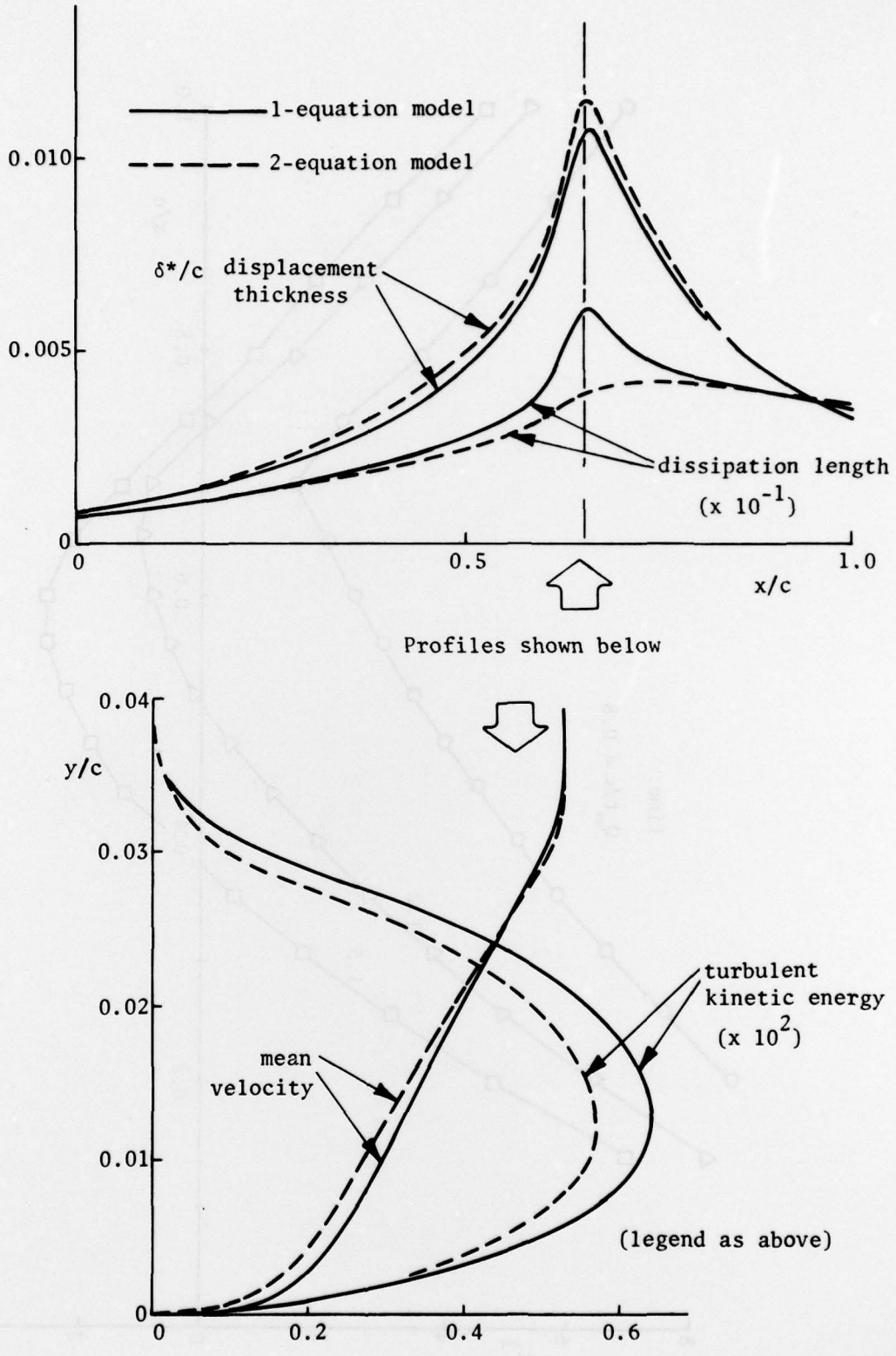

Figure 17 COMPARISON BETWEEN 1- AND 2-EQUATION TURBULENCE MODEL

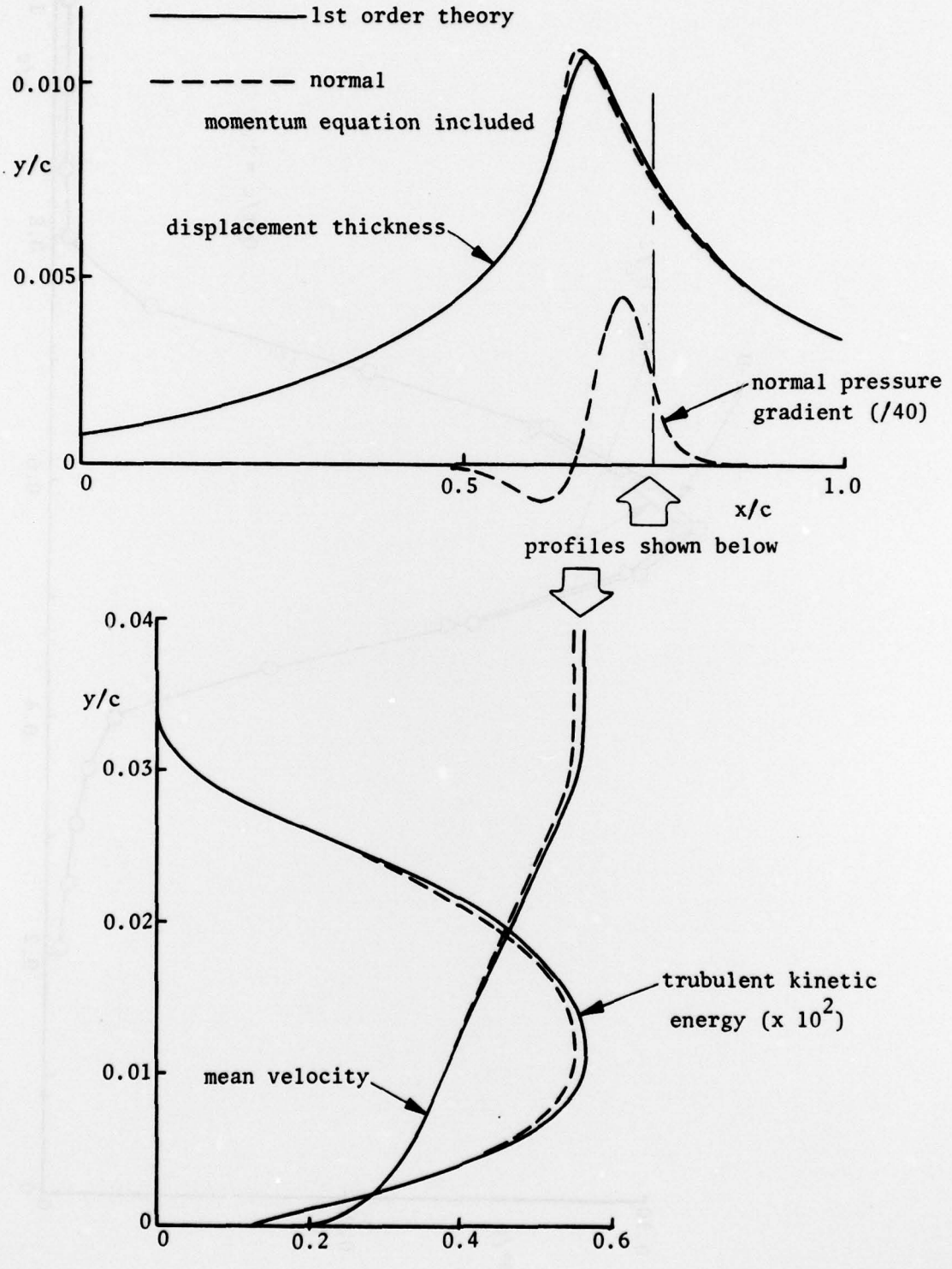

Figure 18 EFFECT OF INCLUDING NORMAL PRESSURE GRADIENTS IN A 2-DIMENSIONAL FLOW

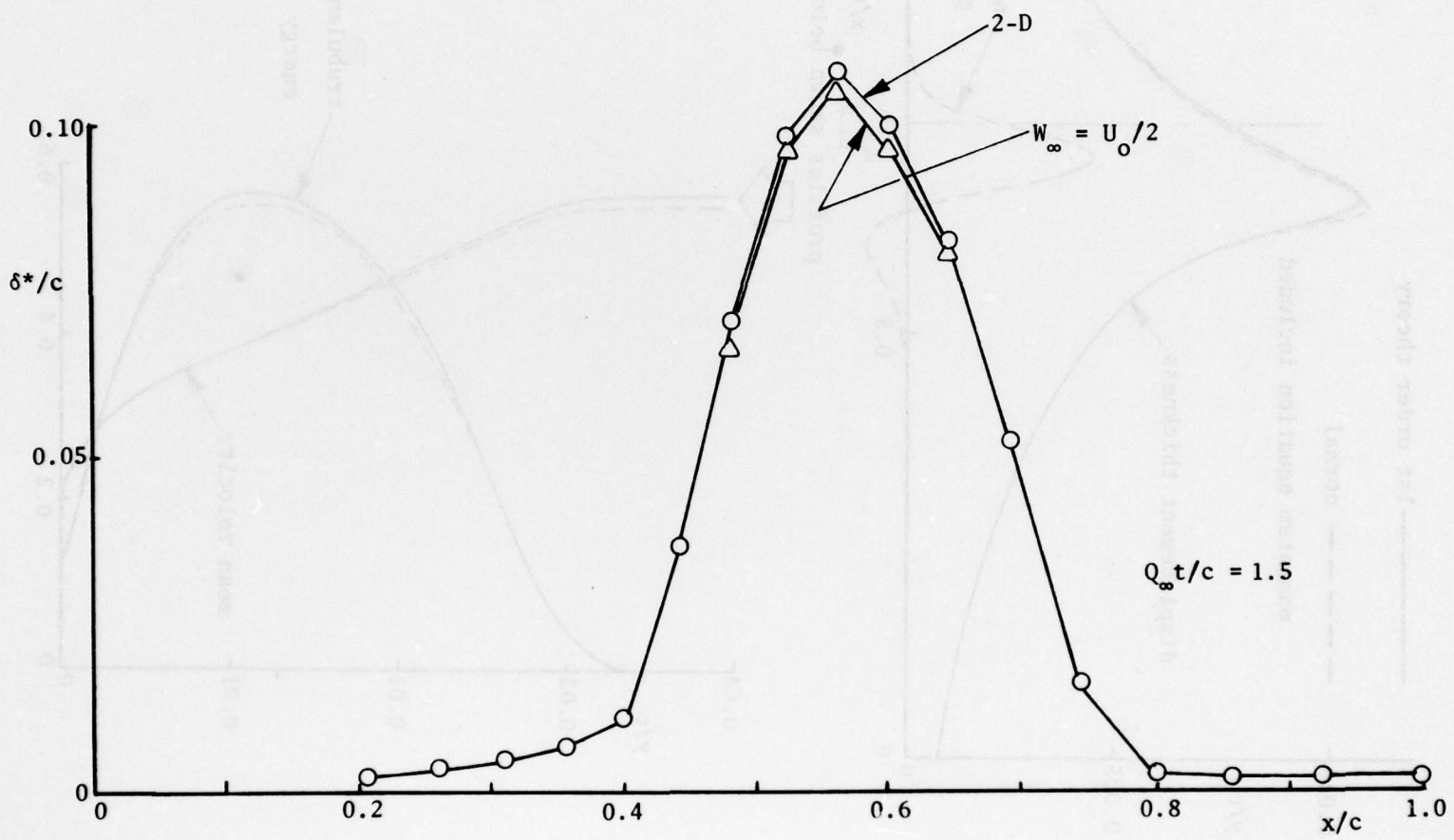

Figure 19 EFFECT OF YAW ON DISPLACEMENT THICKNESS
[M = 0, Turbulent Flow]

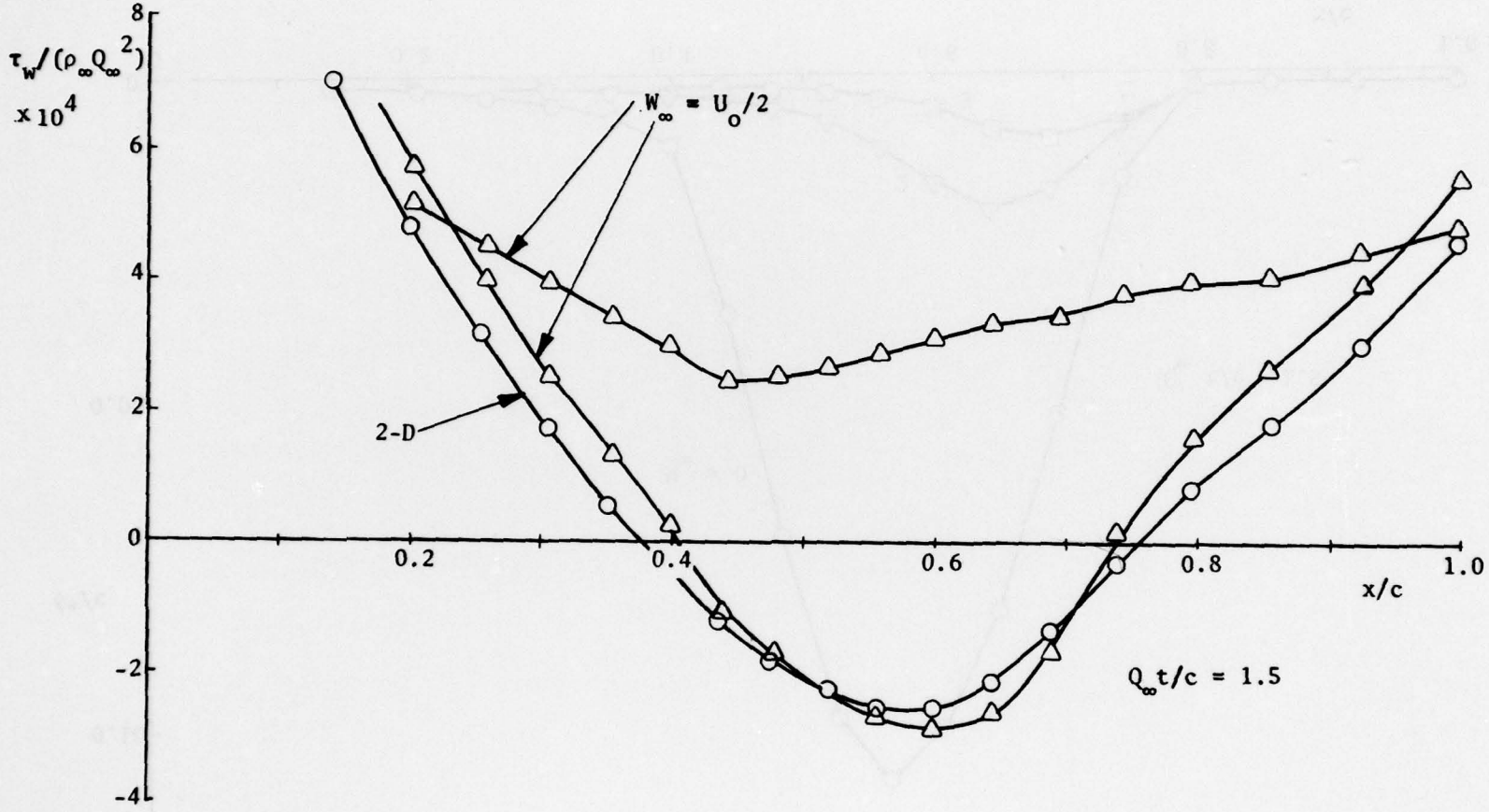

Figure 20 EFFECT OF YAW ON WALL SHEAR STRESS
[M = 0, Turbulent Flow]

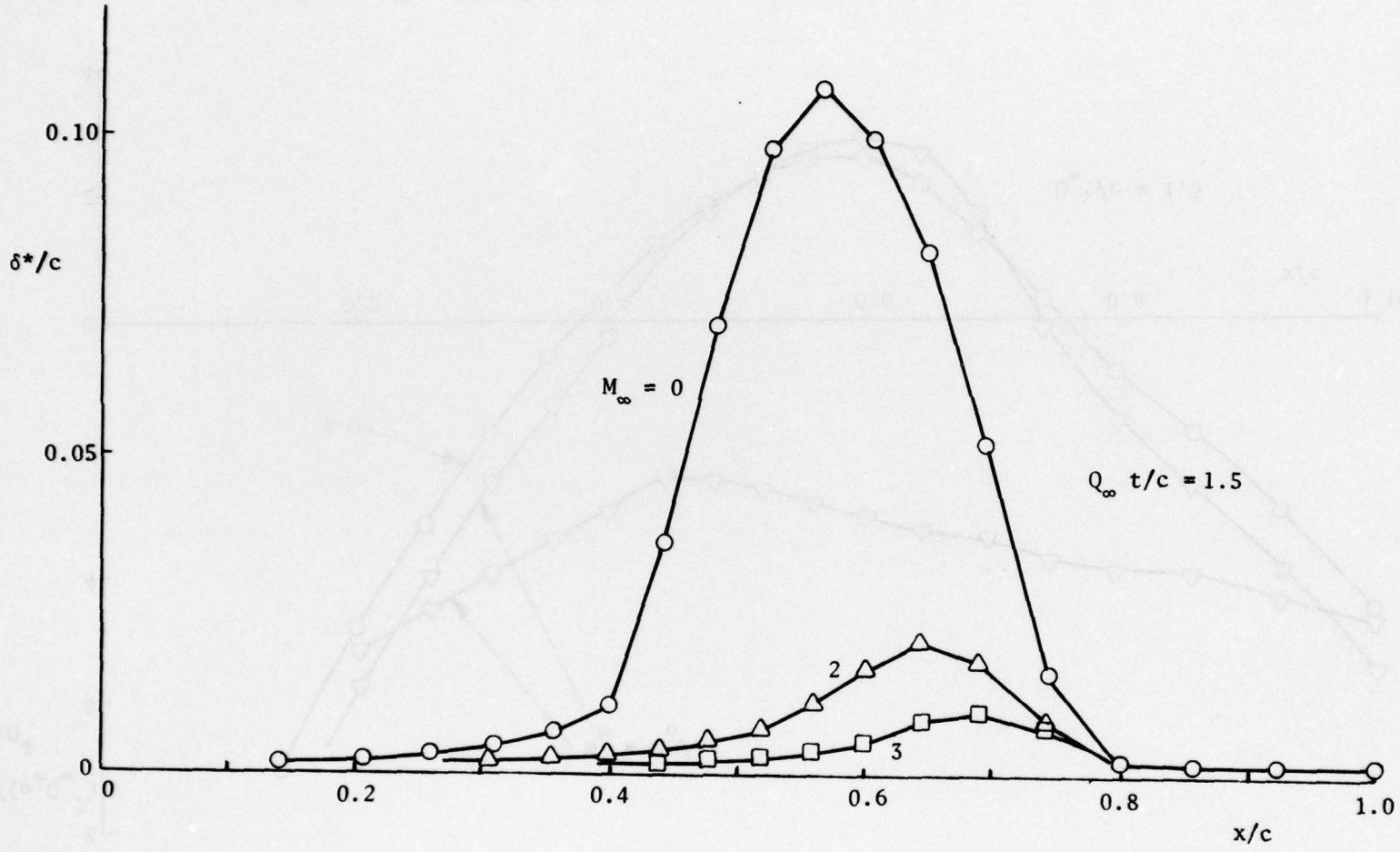

Figure 21 EFFECT OF MACH NUMBER ON DISPLACEMENT THICKNESS
[2-Dimensional Turbulent Flow]

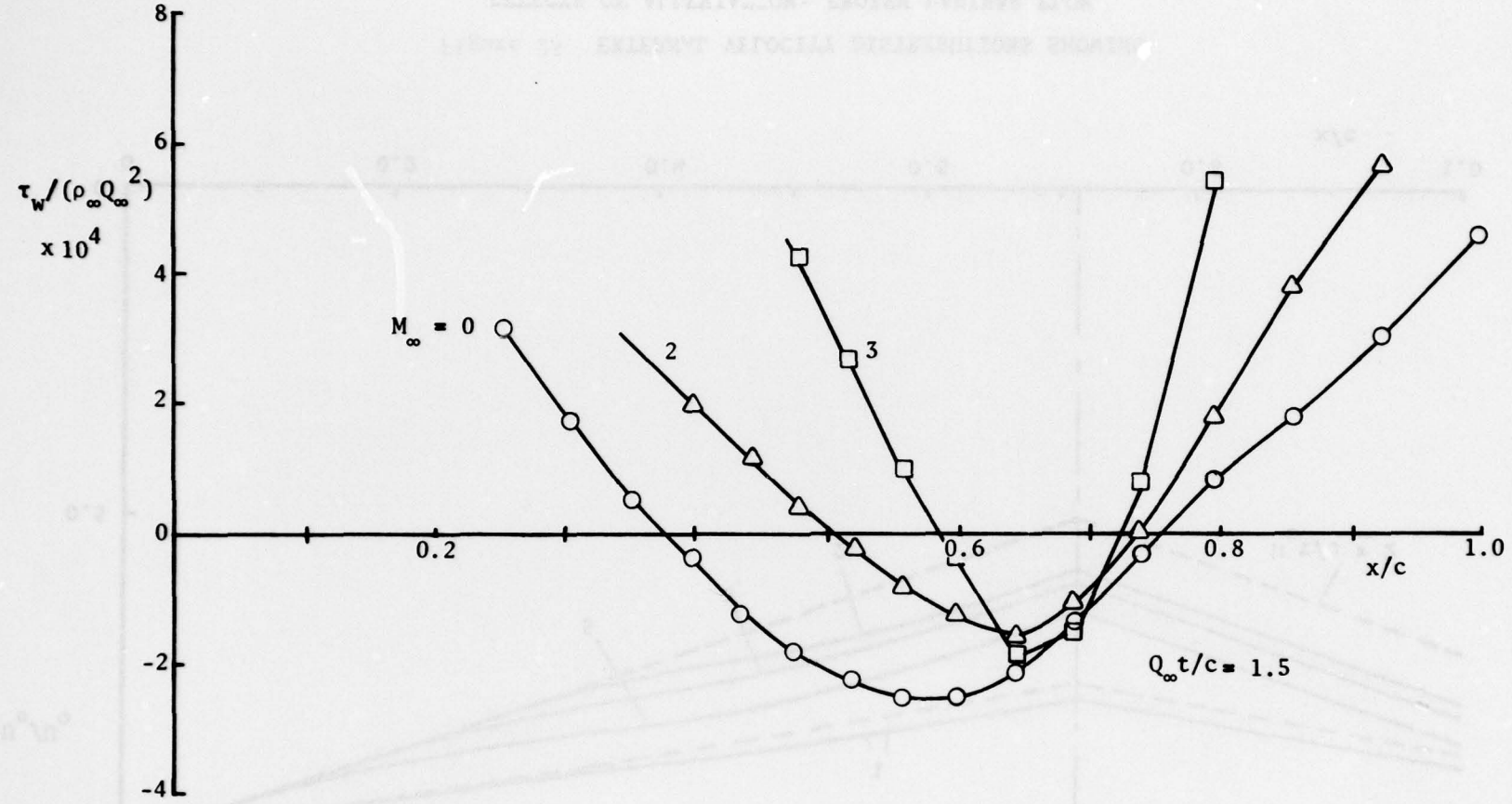

Figure 22 EFFECT OF MACH NUMBER ON WALL SHEAR STRESS
[2-Dimensional Turbulent Flow]

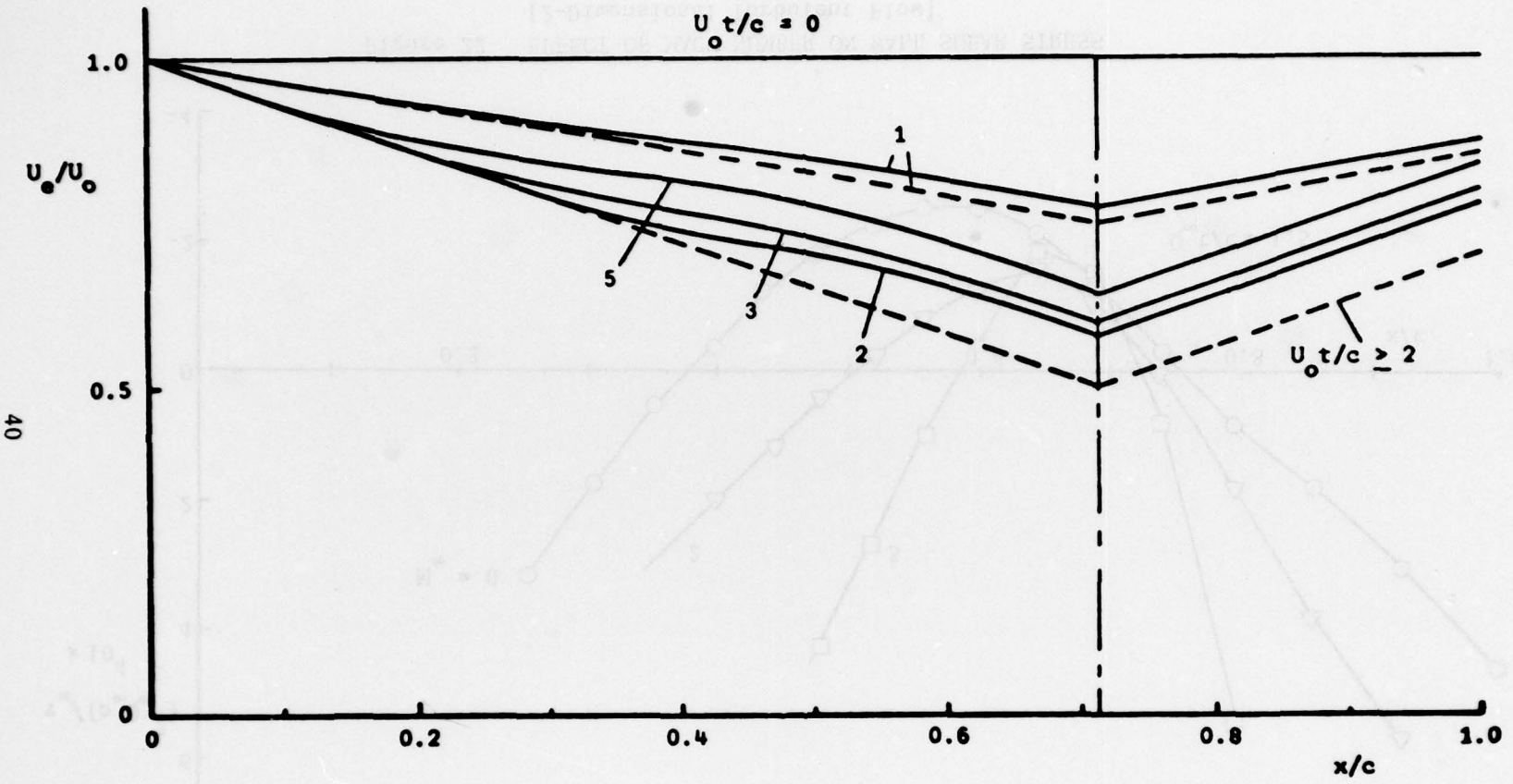

Figure 23 **EXTERNAL VELOCITY DISTRIBUTIONS SHOWING EFFECTS OF ALLEVIATION: FROZEN LAMINAR FLOW**

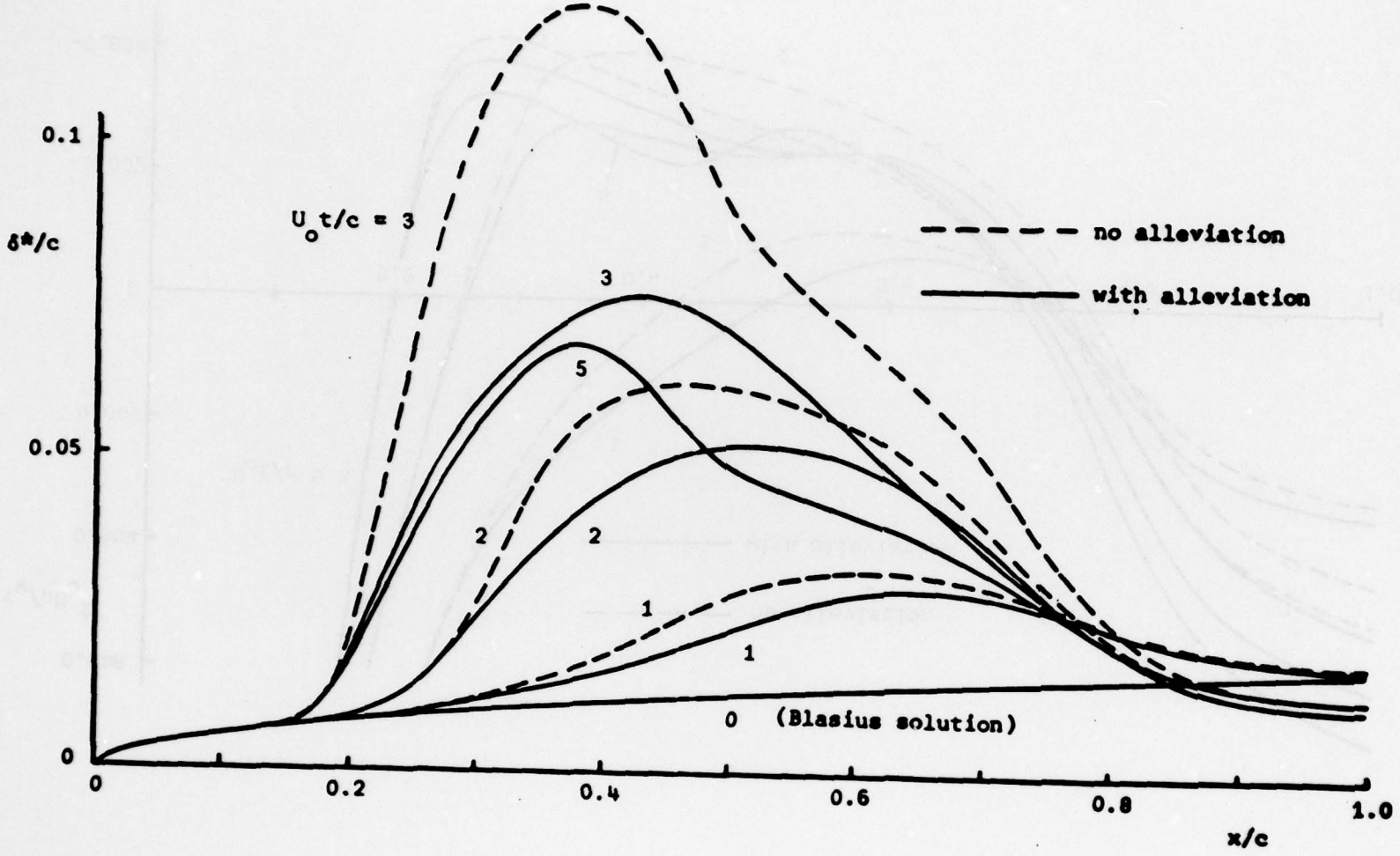

Figure 24 LAMINAR FLOW WITH ALLEVIATION OF PRESSURE GRADIENTS: DISPLACEMENT THICKNESS

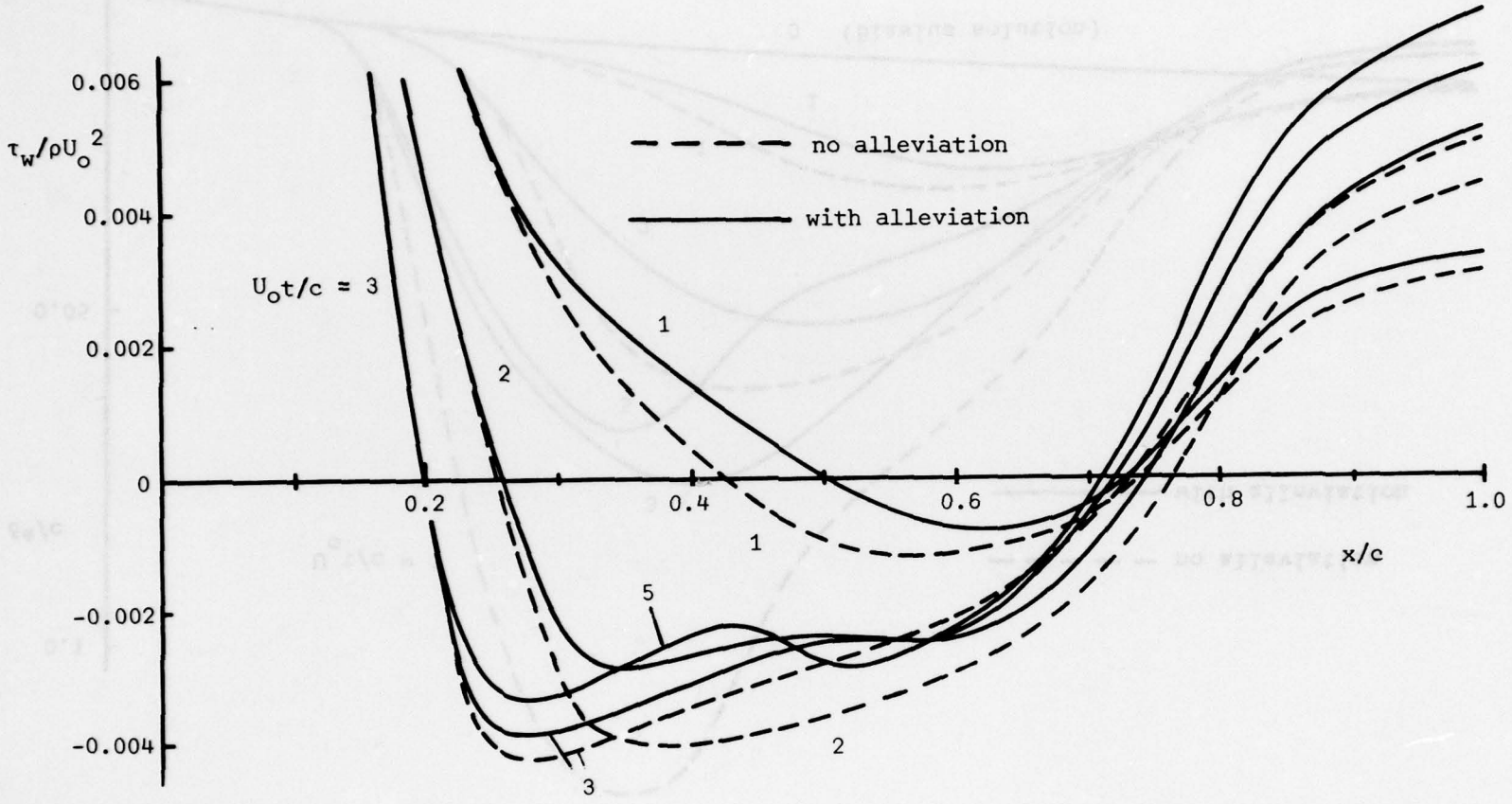

Figure 25 LAMINAR FLOW WITH ALLEVIATION OF PRESSURE GRADIENTS:
WALL SHEAR STRESS

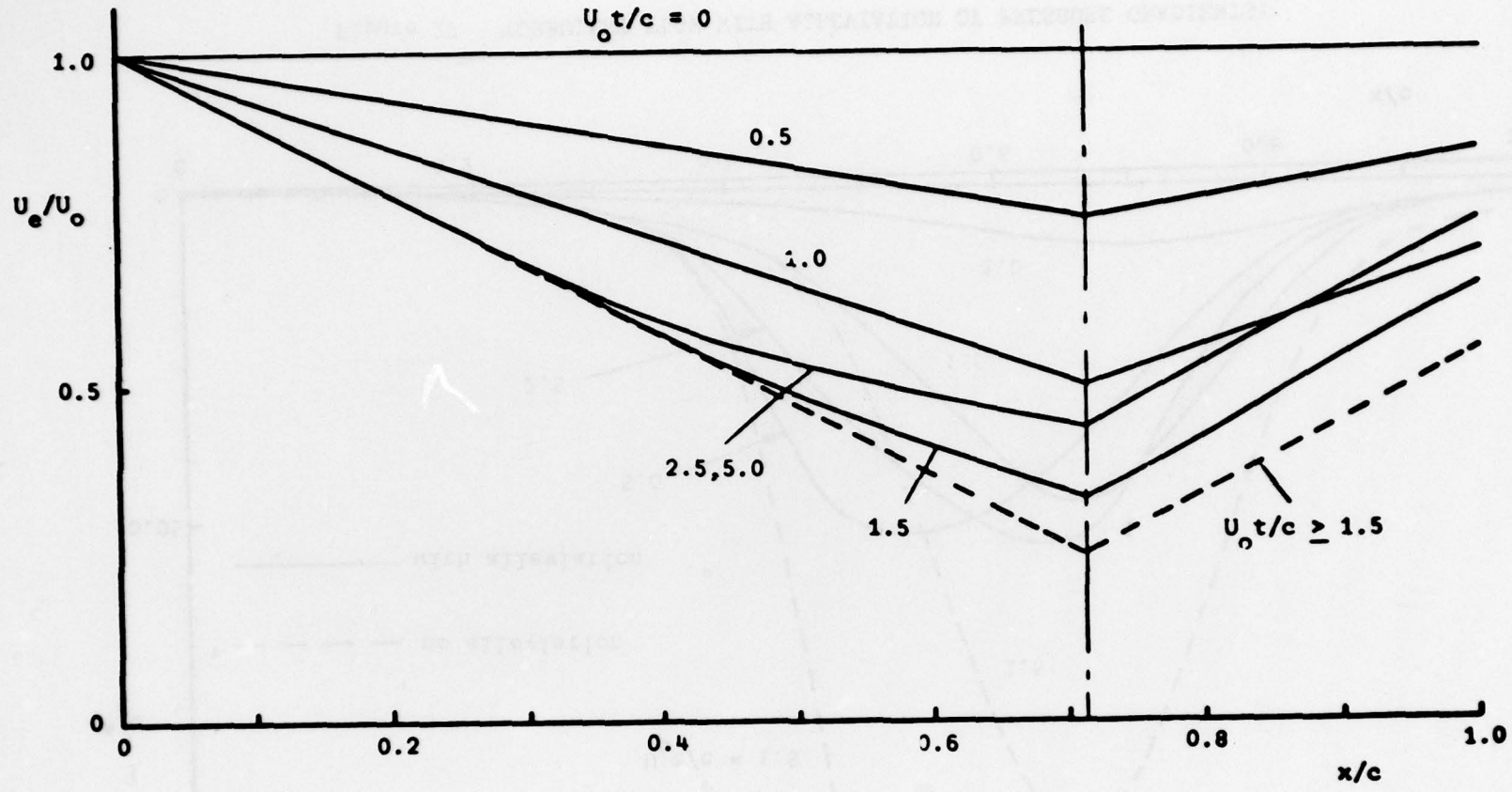

Figure 26 **EXTERNAL VELOCITY DISTRIBUTIONS SHOWING EFFECT OF ALLEVIATION: FROZEN TURBULENT FLOW**

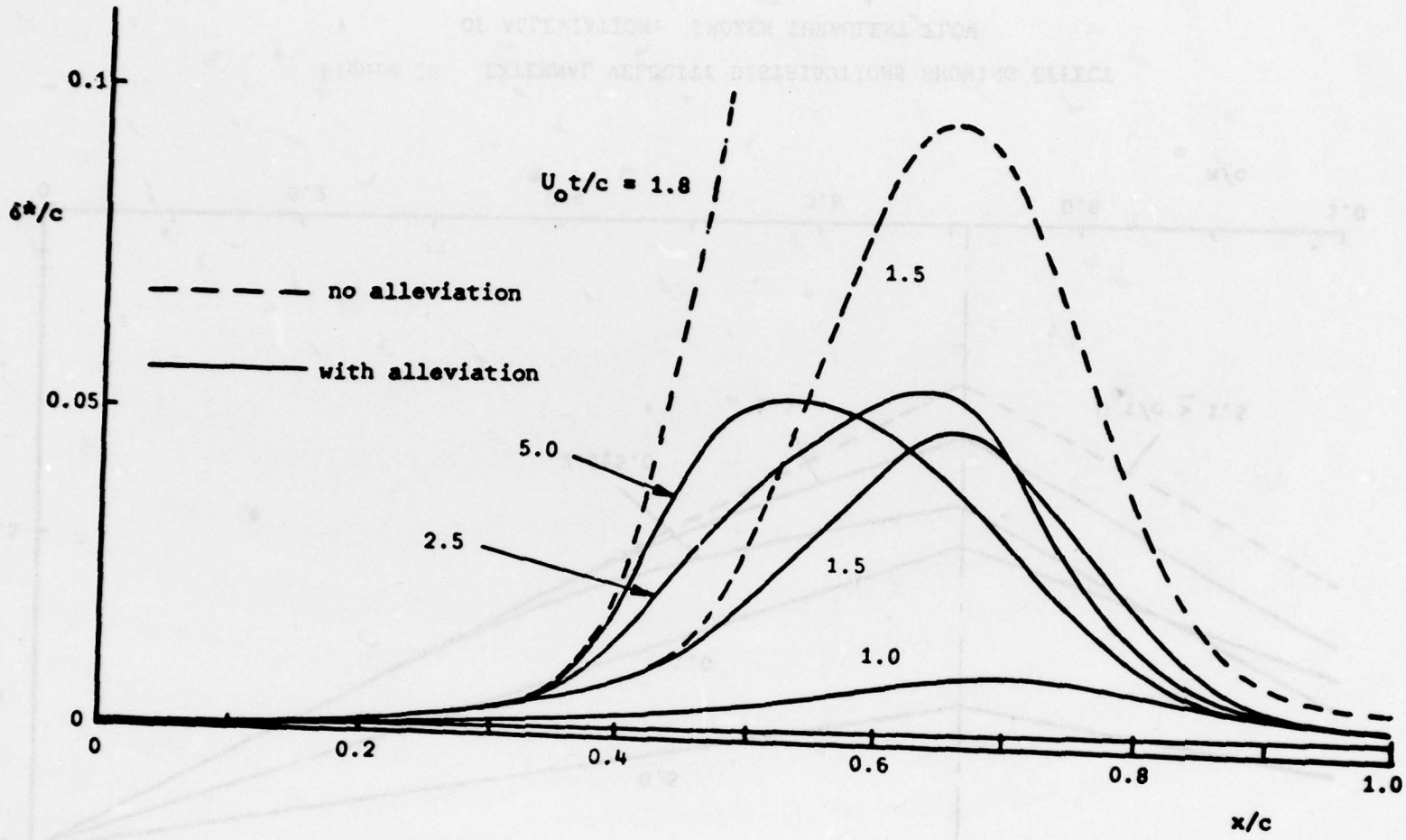

Figure 27 TURBULENT FLOW WITH ALLEVIATION OF PRESSURE GRADIENTS: DISPLACEMENT THICKNESS

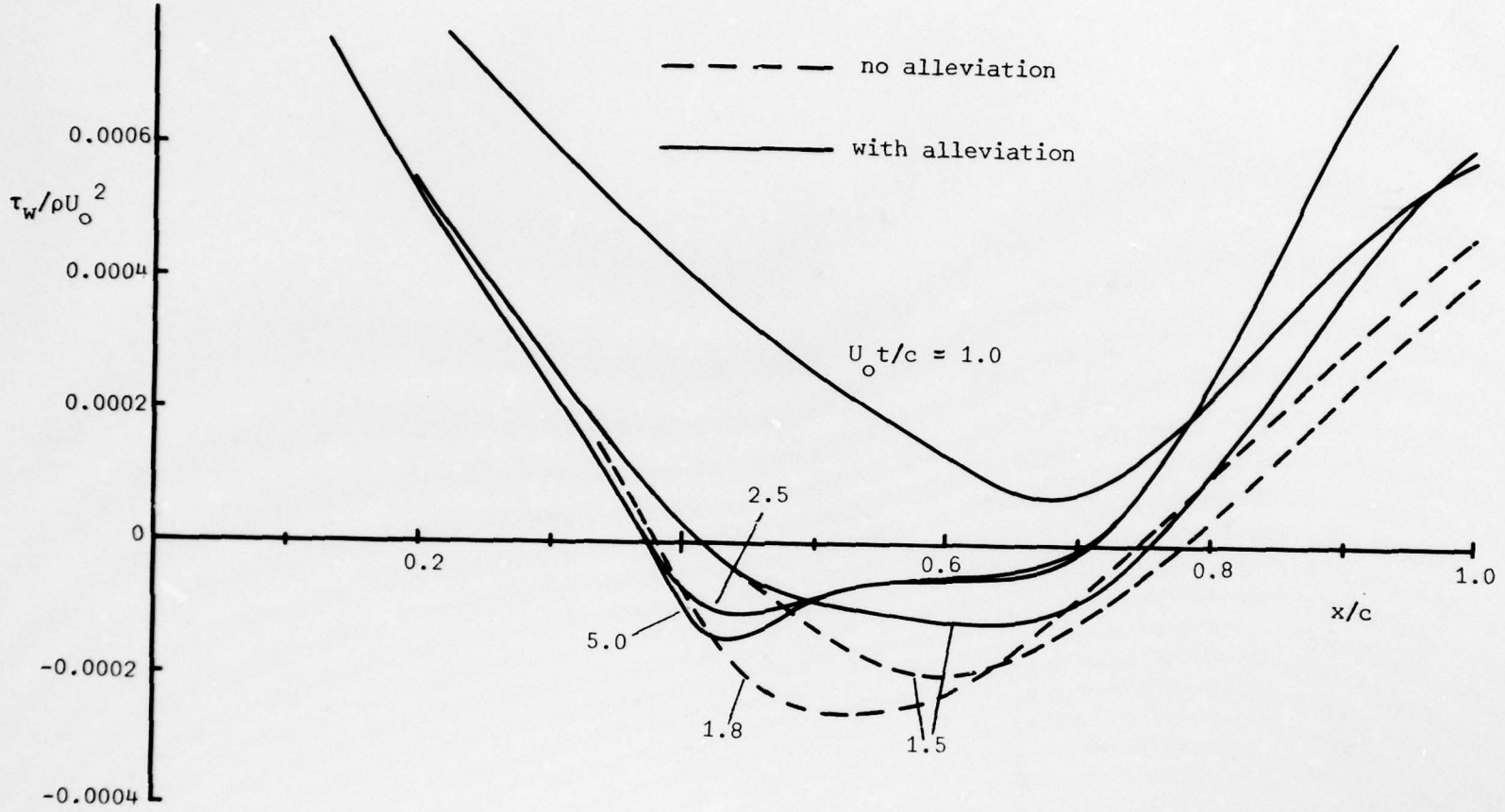

Figure 28 TURBULENT FLOW WITH ALLEVIATION OF PRESSURE GRADIENTS: WALL SHEAR STRESS